# Strain-Controlled Spin Regulation in Fe-N-C Catalysts for Enhanced Oxygen Reduction Reaction Activity

Mingyuan Yu[1,2,3], Jiaxiang Wu[1,2,3], Yashi Chen[4], Yongping Du[1,2,3], Ang Li[1,2,3], Erjun Kan[1,2,3]*, Cheng Zhan[1,2,3]*

[1]School of Physics, Nanjing University of Science and Technology, Nanjing 210094, China

[2]MIIT Key Laboratory of Semiconductor Microstructure and Quantum Sensing, Nanjing University of Science and Technology, Nanjing 210094, China

[3]Engineering Research Center of Semiconductor Device Optoelectronic Hybrid Integration in Jiangsu Province, Nanjing 210094, China

[4]School of Materials Science and Engineering, Nanjing University of Science and Technology, Nanjing 210094, China

*Corresponding author: Erjun Kan, Cheng Zhan

E-mail dress: czhan@njust.edu.cn

**Gibbs free energy calculation at constant potential.**

The four-step proton-coupled electron transfer process in OER and ORR is defined as follows:

$$* + O_2 + H^+ + e^- \rightarrow *OOH\#(S1)$$

$$*OOH + H^+ + e^- \rightarrow *O + H_2O\#(S3)$$

$$*O + H^+ + e^- \rightarrow *OH\#(S2)$$

$$*OH + H^+ + e^- \rightarrow * + H_2O\#(S1)$$

where * represent the catalytic site. The forward arrow indicates OER, and the directional arrow indicates ORR. At U=0V vs. SHE, the free energy of proton-electron pair was set as the chemical potential of $\frac{1}{2}H_2$,[1] and then its free energy at any potential U can be expressed as:

$$G_{H^+}(U) + G_{e^-}(U) = G_{H^+}(U) - e * (4.6 + U) = \frac{1}{2}G_{H_2} - e * U \#(S5)$$

and the $G_{H_2}$ can be calculated by:

$$G_{H_2} = E_{H_2} + E_{ZPE} - T * S + C_p(T) \#(S6)$$

the $E_{H_2}$ was calculated by DFT, $E_{ZPE}$ is zero-point energy obtained from vibration calculation at T = 298.15 K and P = 1 bars. S and $C_p(T)$ is standard entropy and heat capacity taken from thermodynamic table. For liquid water calculations, we consider the chemical potential of liquid water is equal to the chemical potential of water in the gas phase at T = 298.15 K and P = 0.035 bars.[2] Since the energy of $O_2$ cannot be accurately calculated using DFT, we make the following approximation:

$$G_{O_2} = (2G_{H_2O} - 2G_{H_2} - 4.92\ eV) \#(S7)$$

In addition, we also performed thermodynamic corrections on the adsorption state free energy:[3]

$$G(U) = E(U) + E_{ZPE} - T * S \#(S8)$$

Finally, the reaction free energy of OER and ORR can be expressed as:

$$\Delta G_1(U) = G_{*OOH}(U) - [\frac{1}{2}G_{H_2} - e * U + G_*(U) + G_{O_2}] \#(S9)$$

$$\Delta G_2(U) = [G_{*O}(U) + G_{H_2O}] - [\frac{1}{2}G_{H_2} - e * U + G_{*OOH}(U)] \#(S10)$$

$$\Delta G_3(U) = G_{*OH}(U) - [\frac{1}{2}G_{H_2} - e * U + G_{*O}(U)] \#(S11)$$

$$\Delta G_4(U) = [G_*(U) + G_{H_2O}] + [\frac{1}{2}G_{H_2} - e * U + G_{*OOH}(U)] \#(S12)$$

**Formation energy under strain:**

We used formation energy $\Delta E_{form}^{x}$ to evaluate stability of different spin state FeNC under different strain, which is defined as follows:

$$\Delta E_{form}^{x} = E_{FeNC}^{x} - E_{grephene}^{x} + 6 * \mu_C - 4 * \mu_N - \mu_{Fe} \#(S13)$$

where $E_{FeNC}^{x}$ and $E_{graphene}^{x}$ is the total energy of the FeNC and graphene substrate under x% stain, receptivity. $\mu_C$, $\mu_N$ and $\mu_{Fe}$ are chemical potentials of carbon (graphite), nitrogen ($N_2$) and iron (bulk Fe), respectively.

**Micro-kinetic method:**

Inspired by previous study[4], we constructed a microkinetic model for the OER and ORR process over Fe-N-C SACs. We assume that the reaction occurs with bare $FeN_4$ and $FeN_4$ with one coordination, and the reaction rate at the site is described by the reaction rate of the rate-limiting step. Therefore, the reaction rate can be written as:

$$R(U) = \sum k_i(U)[C_i(U)] \#(S13)$$

$$k_i(U) = A_i \exp(\frac{-E_{a,i}}{k_B T}) \exp\left(\frac{-G_i^b(U)}{k_B T}\right) \#(S14)$$

R(U) is the total reaction rate, $C_i(U)$ is the concentration of various possible active sites. $A_i$, $E_{a,i}$ are effective pre-exponential factor and activation energy, which can be estimated to be 0.26 eV and $1.23\times10^9$ $s^{-1}$.[5, 6] $k_B$ is Boltzmann constant. $k_i(U)$ are the reaction rates in corresponding active sites. This can be computed from Eq. S14, based on classical transition theory. $G_i^b(U)$ is the reaction barrier. In addition, the concentration $C_i(U)$ is balanced according to total site concentration following the formula:

$$[M] = \sum [C_i(U)] \#(S15)$$

where M is total concentration of active sites, which can be computed by active sites divided by surface area. Besides, $C_i(U)$ follow the equilibrium constants:

$$K_i(U) = \frac{C_i(U)}{C_0(U)} = \exp\left(\frac{-G_i^f(U)}{kT}\right) \#(S16)$$

$C_0(U)$ is concentration of $FeN_4^{IS}$, the $G_i^b(U)$ is formation energy of various active site relative to $FeN_4^{IS}$. Finally, the current density can be calculated as:

$$j(U) = \frac{nFR(U)}{N_A} \#(S17)$$

Where n is the charge transfer of reaction, F is Faraday constant, and $N_A$ is the Avogadro constant. It should be noted that there is a limit to the reaction rate of ORR due to the solubility limit of oxygen[7]. The reaction rate changes to:

$$k_i(U) = \exp\left(\frac{-E_{a,i}}{k_B T}\right) min(A_i exp\left(\frac{-G_i^b(U)}{k_B T}\right), v_{O_2}) \#(S18)$$

The values of $v_{O_2}$ is taken as $1\times10^8$ $s^{-1}$.[8]

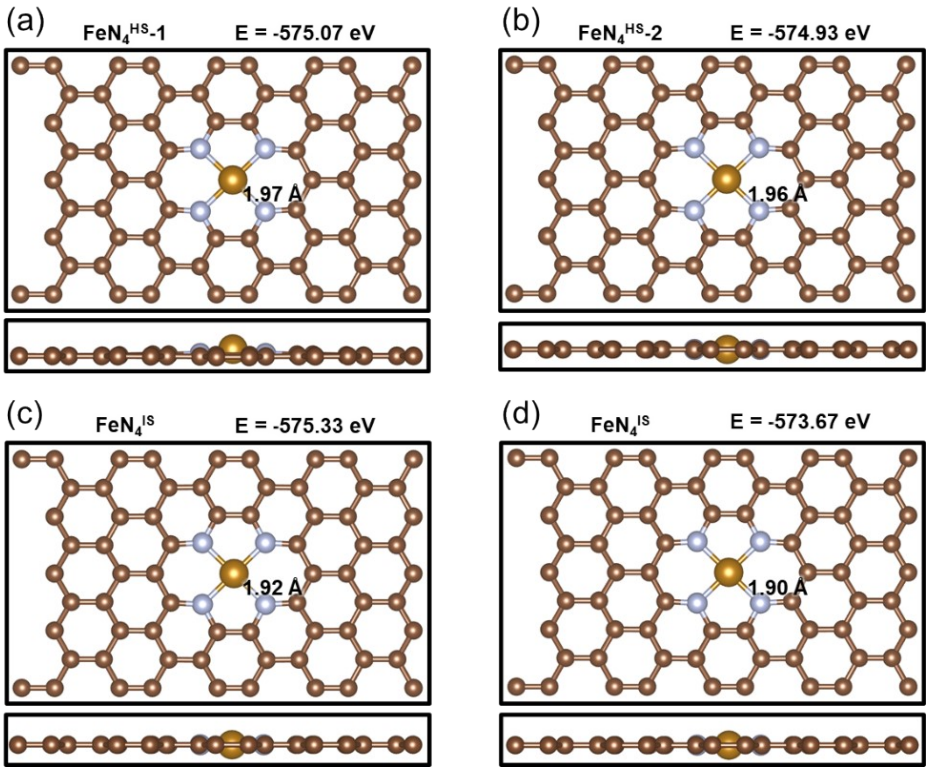


**Fig. S1** The structure of (a) $FeN_4^{HS}$-1, (b) $FeN_4^{HS}$-2, (c) $FeN_4^{IS}$, and (d) $FeN_4^{LS}$. (E: electronic free energy of structure; insert: Fe-N bond length)

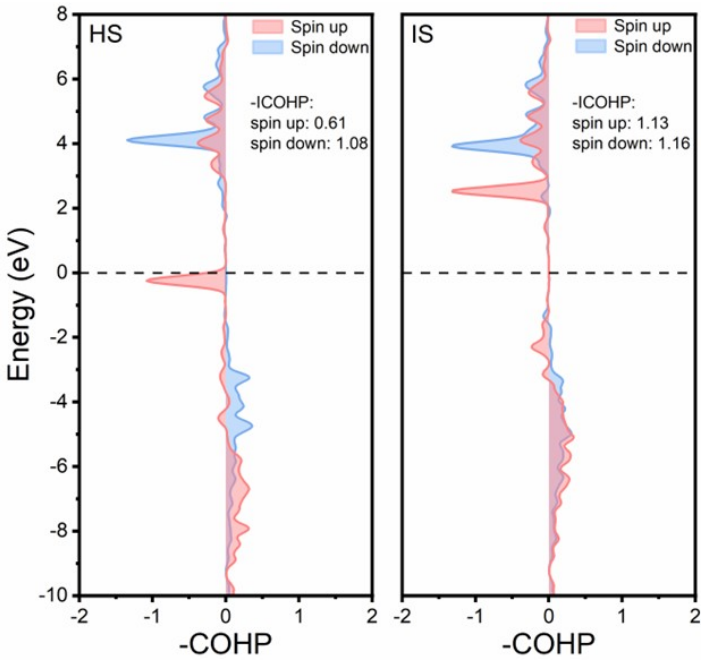


**Fig. S2** COHP analyze for the Fe-N bond with HS/IS in $FeN_4$.

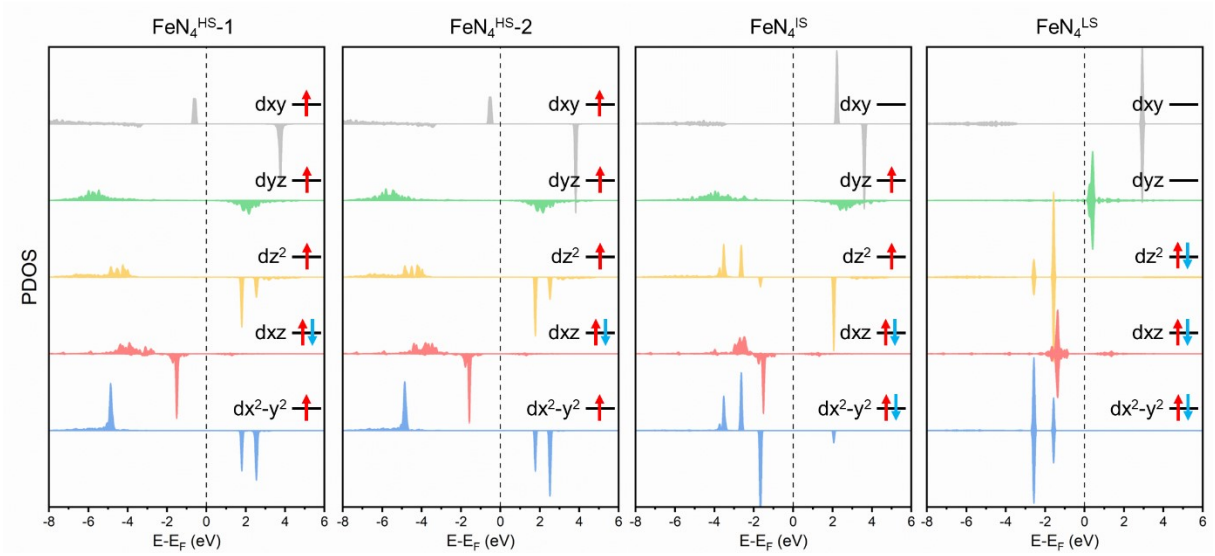


**Fig. S3** PDOS of $FeN_4^{HS}$-1, $FeN_4^{HS}$-2, $FeN_4^{IS}$ and $FeN_4^{LS}$.

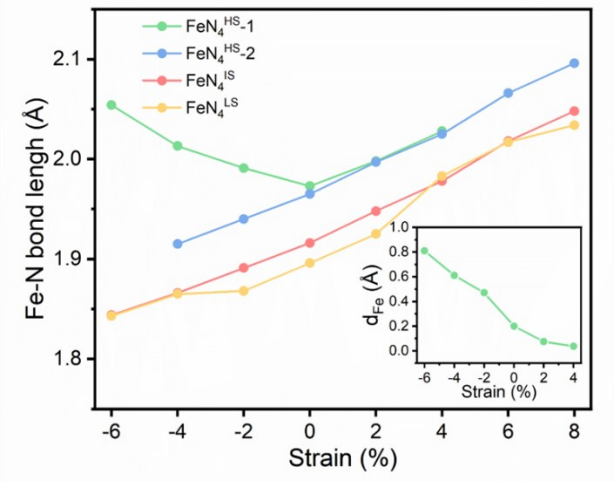


**Fig. S4** (a) Fe-N bond length of different structure of Fe-N-C under strain from -6 % to 8 % (insert: out-plane displacement of Fe refers to N in $FeN_4^{HS}$-1).

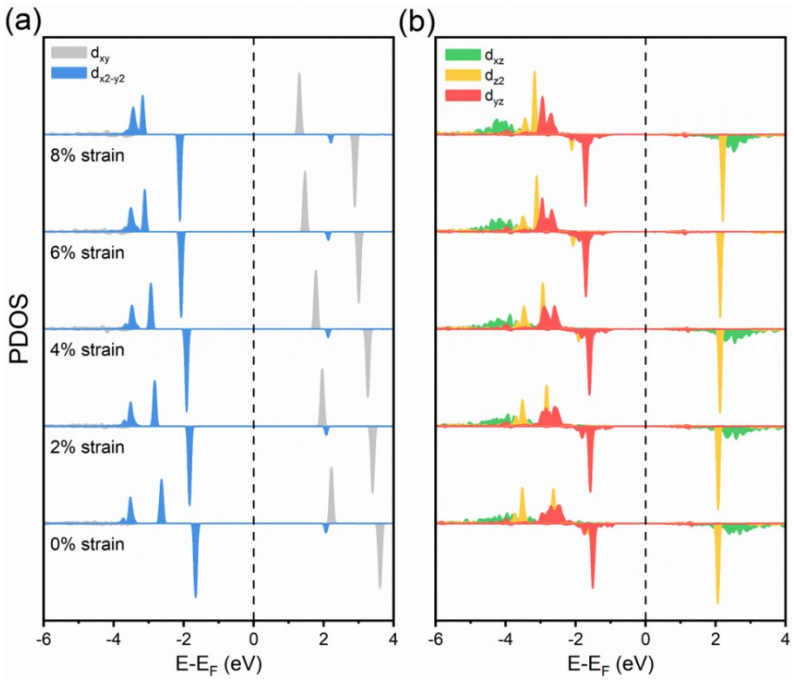


**Fig. S5** The PDOS of $FeN_4^{IS}$ under different strain. (a) $d_{xy}$ and $d_{x2-y2}$, (b) $d_{xz}$, $d_{z2}$, and $d_{yz}$.

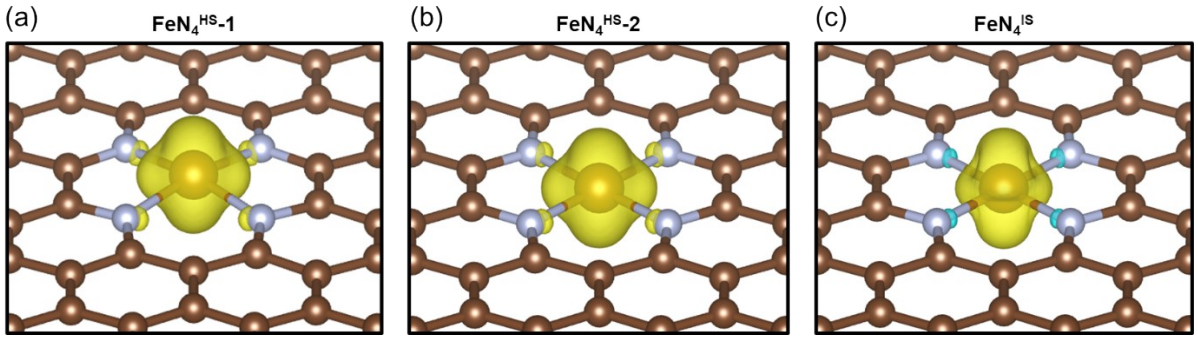


**Fig. S6** Spin density of (a) $FeN_4^{HS}$-1, (b) $FeN_4^{HS}$-2, (c) $FeN_4^{IS}$. (Isosurface: 0.01e/ bohr$^3$)

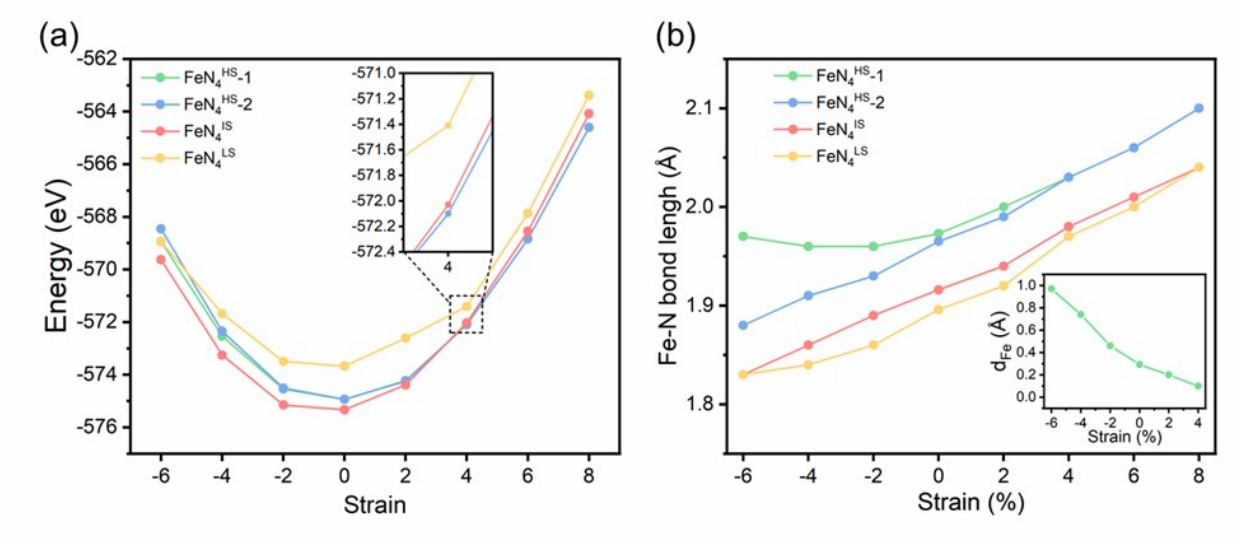


**Fig. S7** (a) Free energy of different spin state of Fe-N-C under strain from -6 % to 8 % along the y-direction. (b) Fe-N bond length of different structure of Fe-N-C under strain from -6 % to 8 % (insert: out-plane displacement of Fe refers to N in $FeN_4^{HS}$-1).

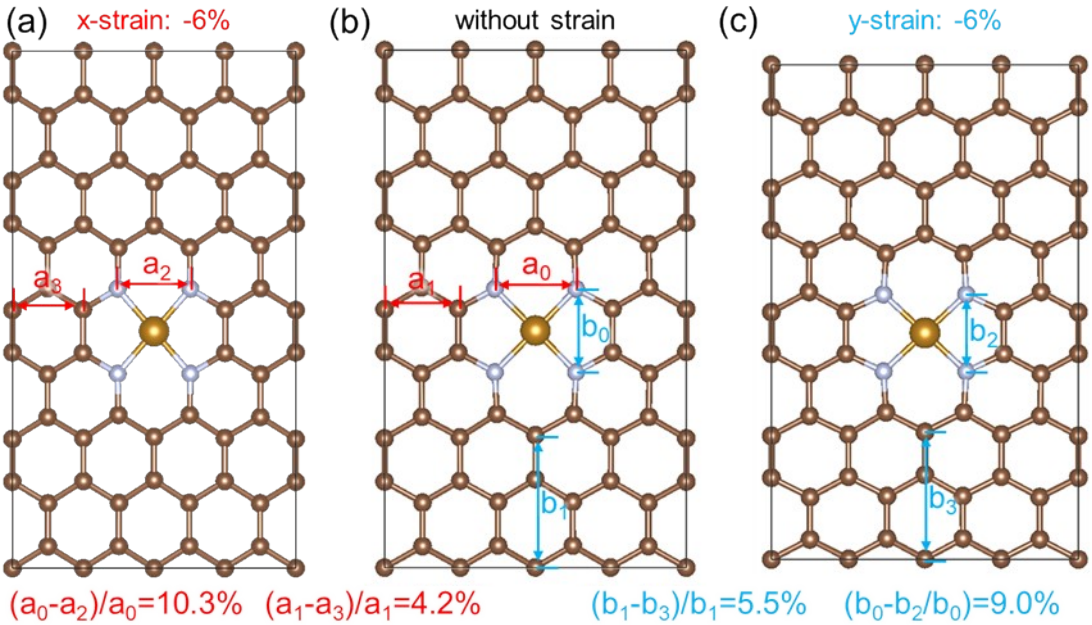


**Fig. S8** IS state of $FeN_4$ (a) under -6% strain in x direction, (b) without strain, (c) under -6% strain in y direction.

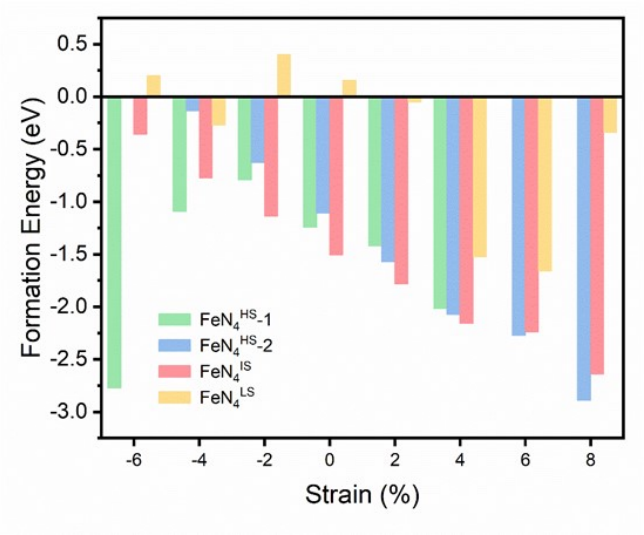


**Fig. S9** Formation energy of $FeN_4$ with different spin state under strain.

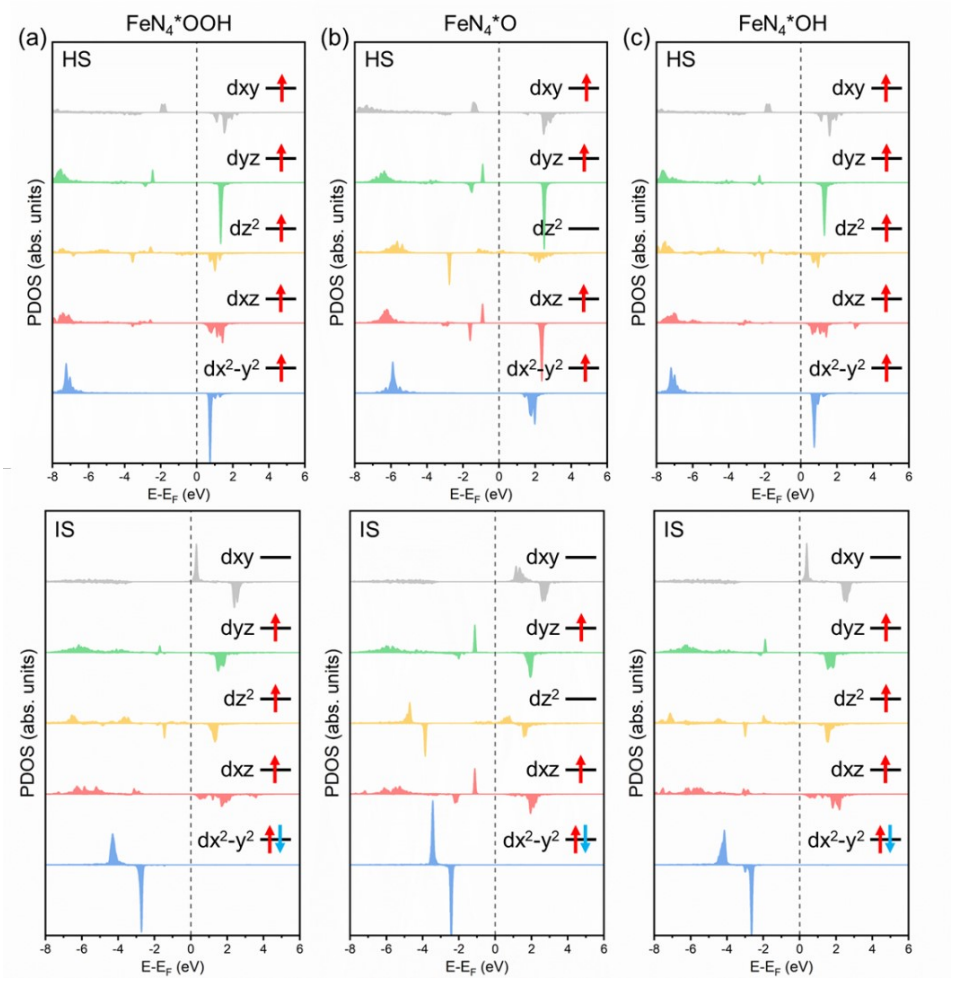


**Fig. S10** PDOS and electron occupation diagram of HS (up) and IS (down). (a) $FeN_4$*OOH, (b) $FeN_4$*O, (c) $FeN_4$*OH.

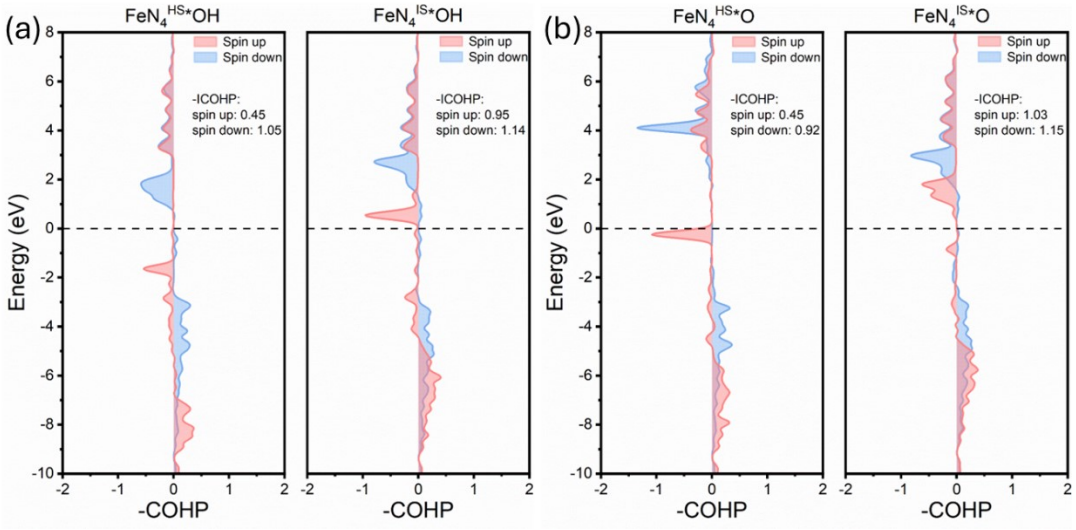


**Fi g. S11** COHP analyze for the Fe-N bond in (a) $FeN_4^{HS/IS}$*OH, (b) $FeN_4^{HS/IS}$*O.

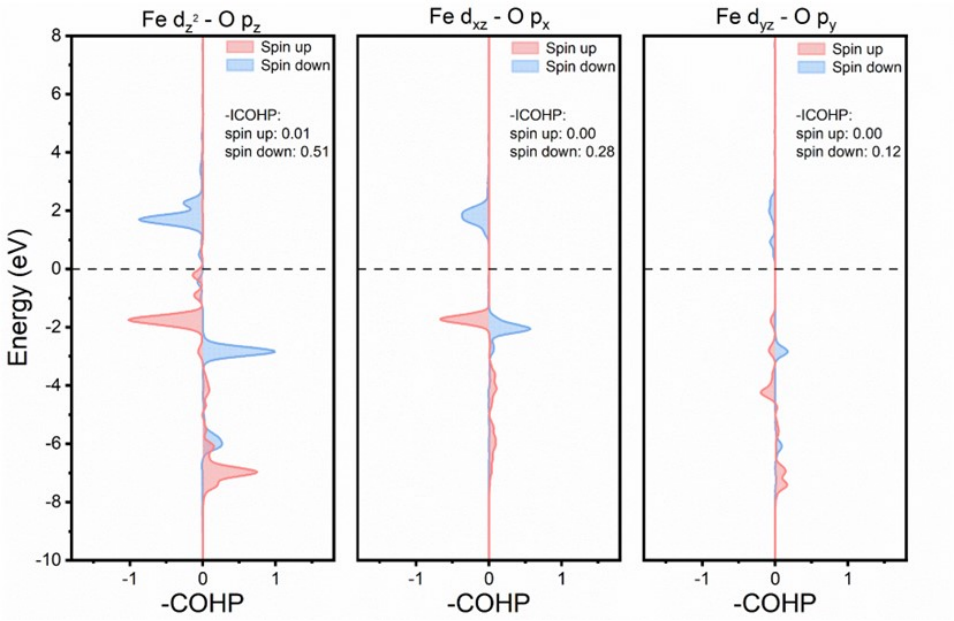


**Fig. S12** Orbital resolved COHP analyze for the Fe-O bond in $FeN_4^{IS}$*OH.

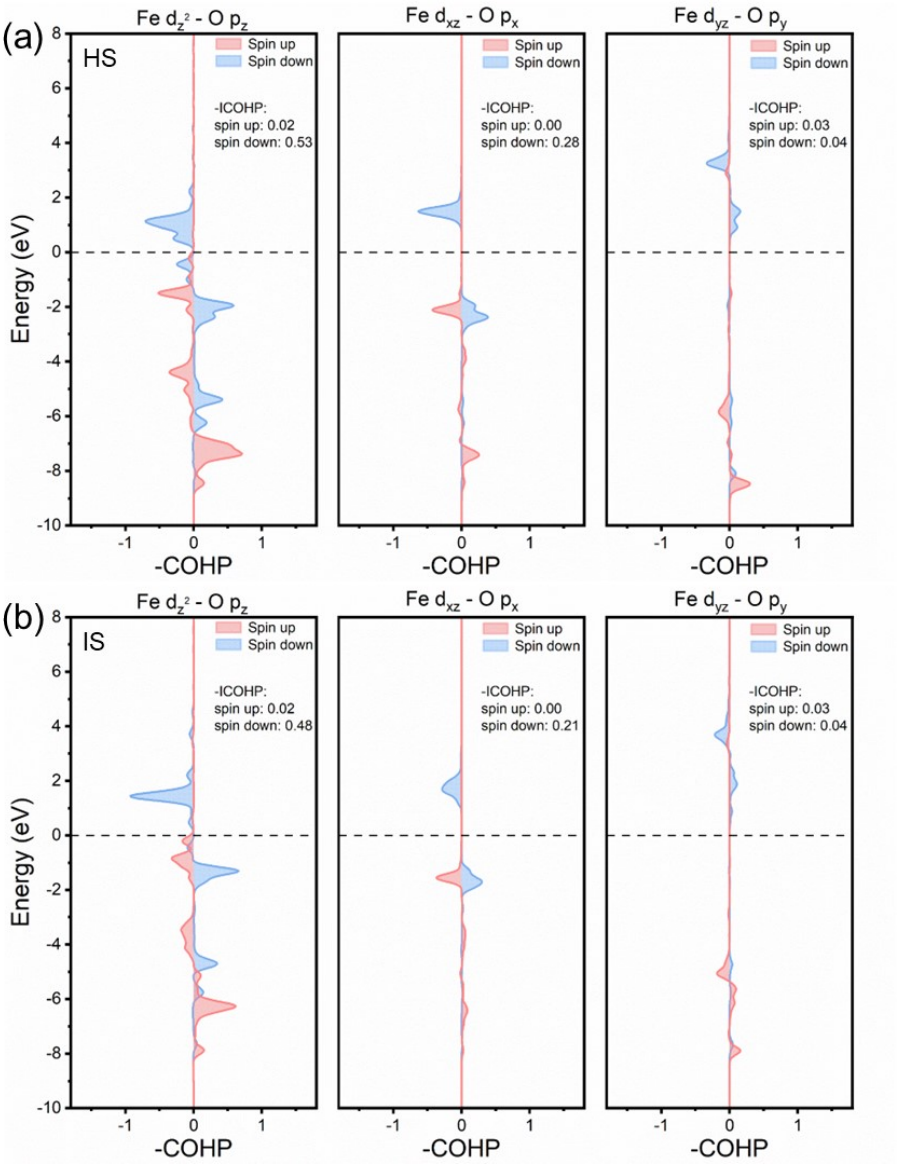


**Fig. S13** Orbital resolved COHP analyze for the Fe-O bond in $FeN_4$*OOH. (a) HS, (b) IS.

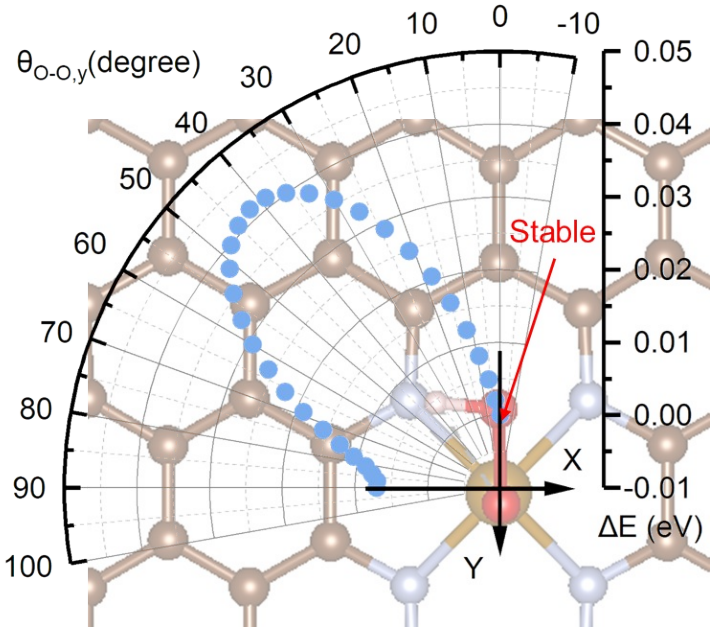


**Fig. S14** Energy variation as a function of the rotation of the HO-O-Fe-N dihedral angle; the labeled /$\theta_{O\text{-}O,y}$ denotes the angle between the O−O bond and the *y*-axis within the *xy* plane.

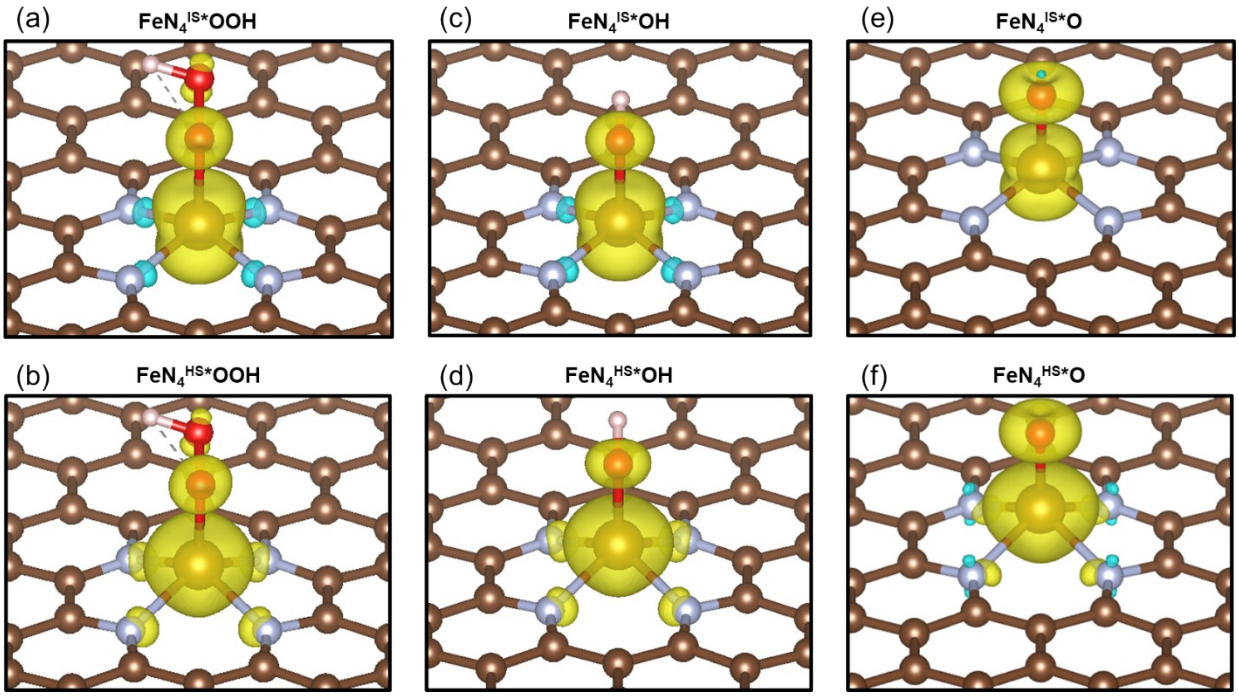


**Fig. S15** Spin density of (a) $FeN_4^{IS}$*OOH, (b) $FeN_4^{HS}$*OOH, (c) $FeN_4^{IS}$*O, (d) $FeN_4^{HS}$*O, (e) $FeN_4^{IS}$*OH, (f) $FeN_4^{HS}$*OH. (Isosurface: 0.01e/ $bohr^3$)

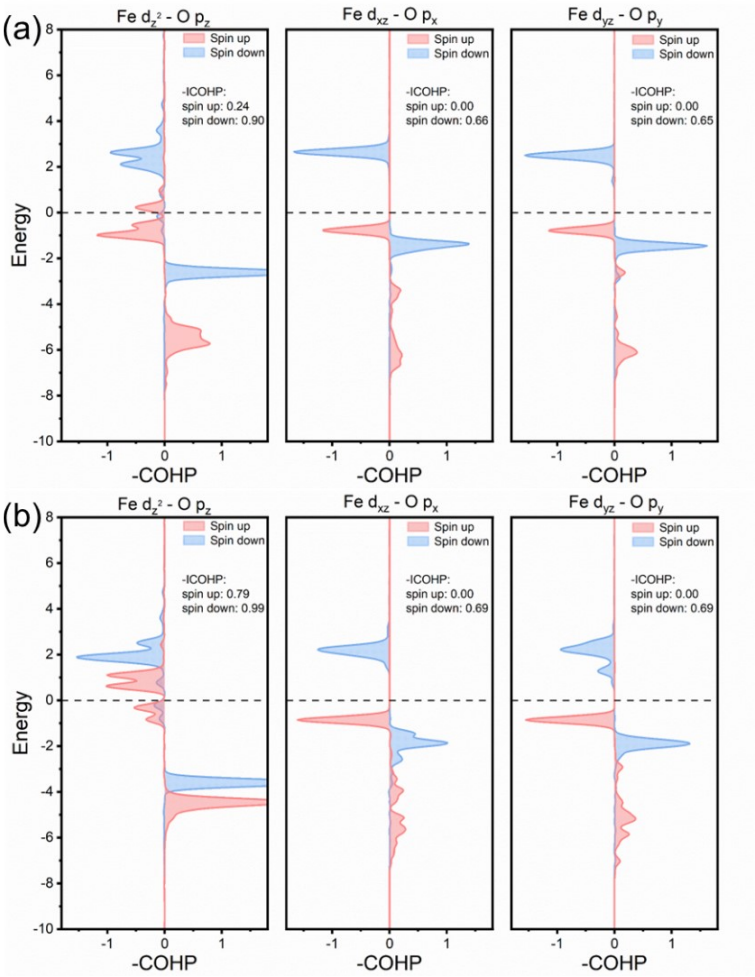


**Fig. S16** Orbital resolved COHP analyze for the Fe-O bond in $FeN_4$*O. (a) HS, (b) IS.

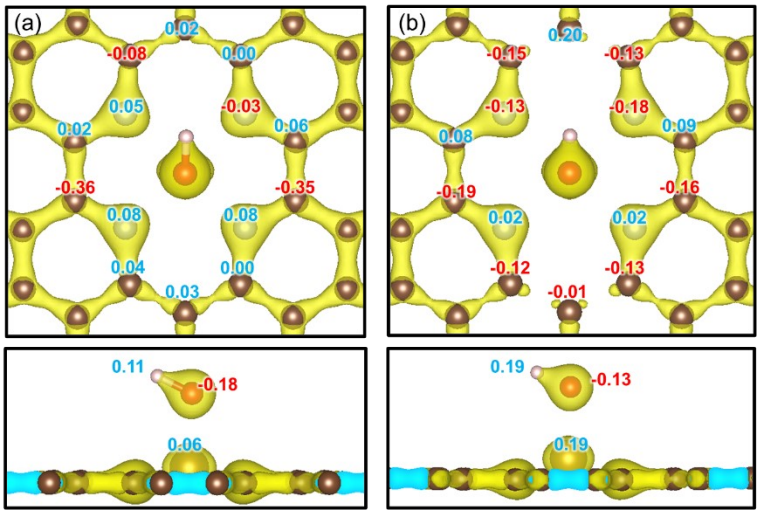


**Fig. S17** Charge density of $FeN_4^{IS}$*OH under (a) 4% strain and (b) 8% strain and Bader charge refer to 0% strain.

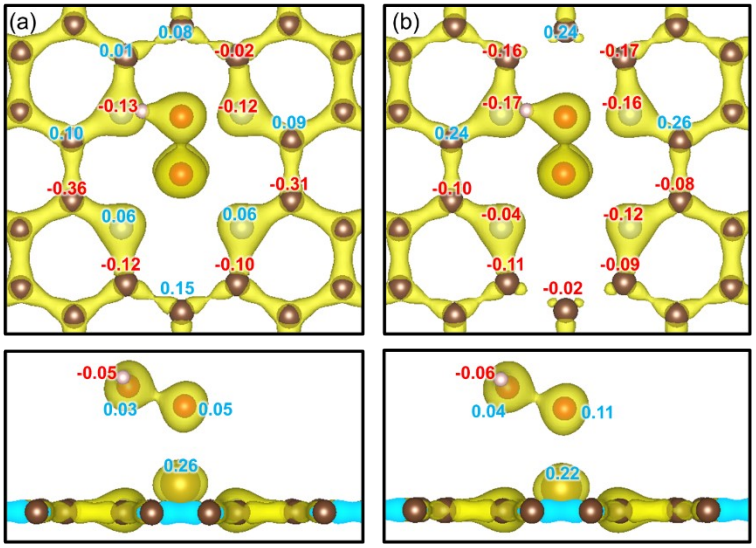


**Fig. S18** Charge density of $FeN_4^{IS}$*OOH under (a) 4% strain and (b) 8% strain and Bader charge refer to 0% strain.

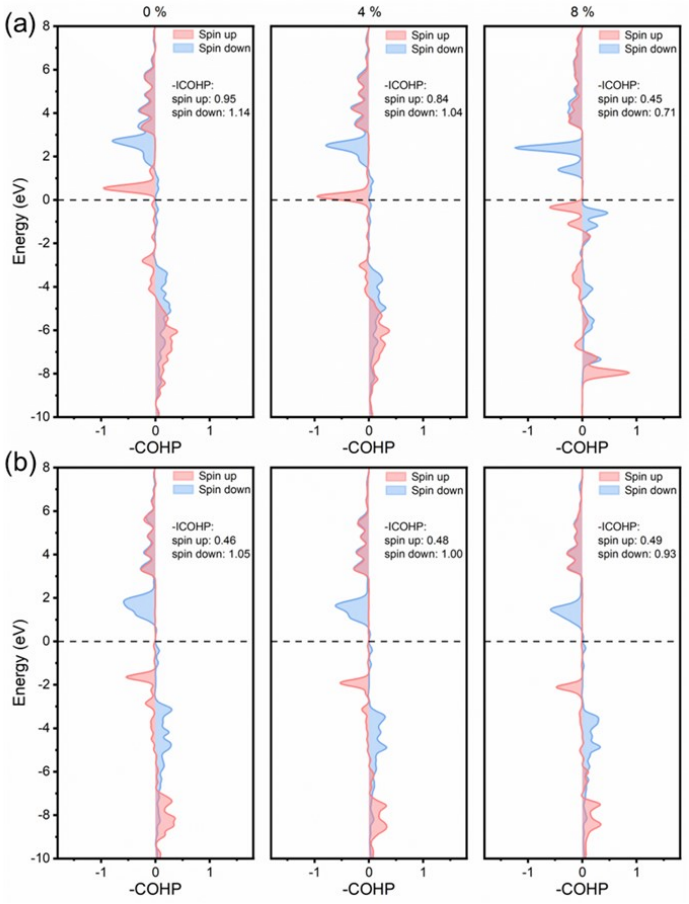


**Fig. S19** Charge density of $FeN_4^{IS}$*OOH under (a) 4% strain and (b) 8% strain and Bader charge refer to 0% strain.

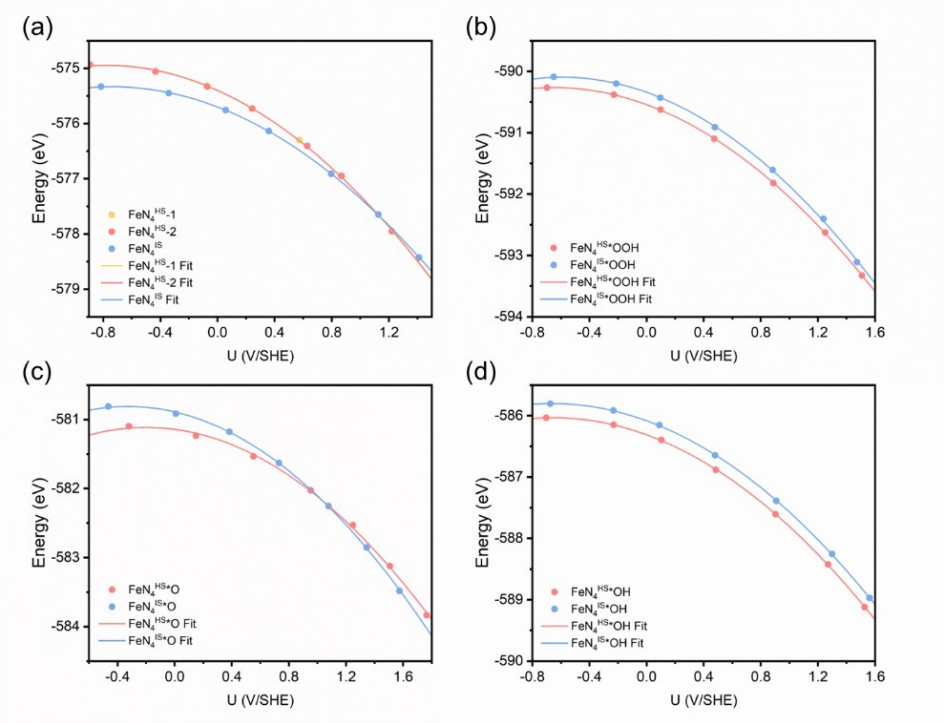


**Fig. S20** Potential-dependent free energy of different spin state of (a) bare $FeN_4$, (b) $FeN_4$*OOH, (c) $FeN_4$*O and (d) $FeN_4$*OH under 0% strain.

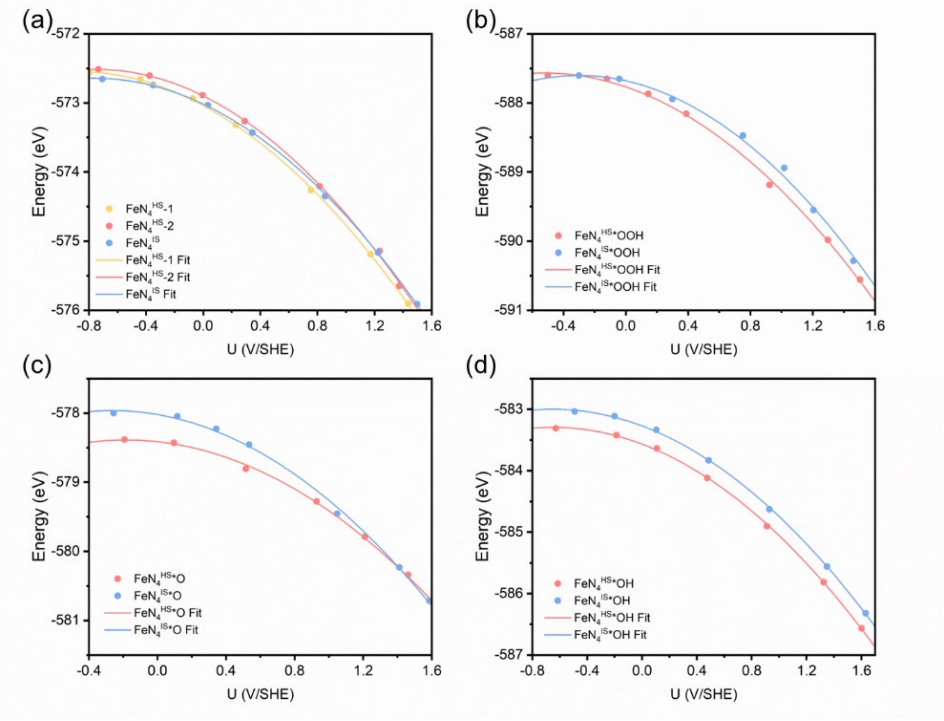


**Fig. S21** Potential-dependent free energy of different spin state of (a) bare $FeN_4$, (b) $FeN_4$*OOH, (c) $FeN_4$*O and (d) $FeN_4$*OH under 4% strain.

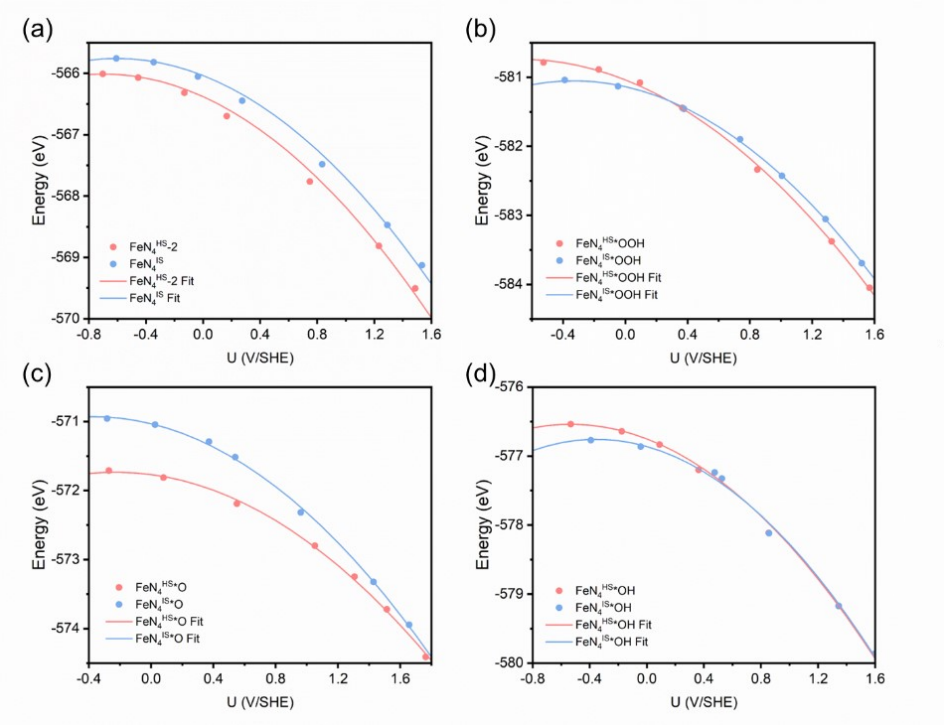


**Fig. S22** Potential-dependent free energy of different spin state of (a) bare $FeN_4$, (b) $FeN_4$*OOH, (c) $FeN_4$*O and (d) $FeN_4$*OH under 8% strain.

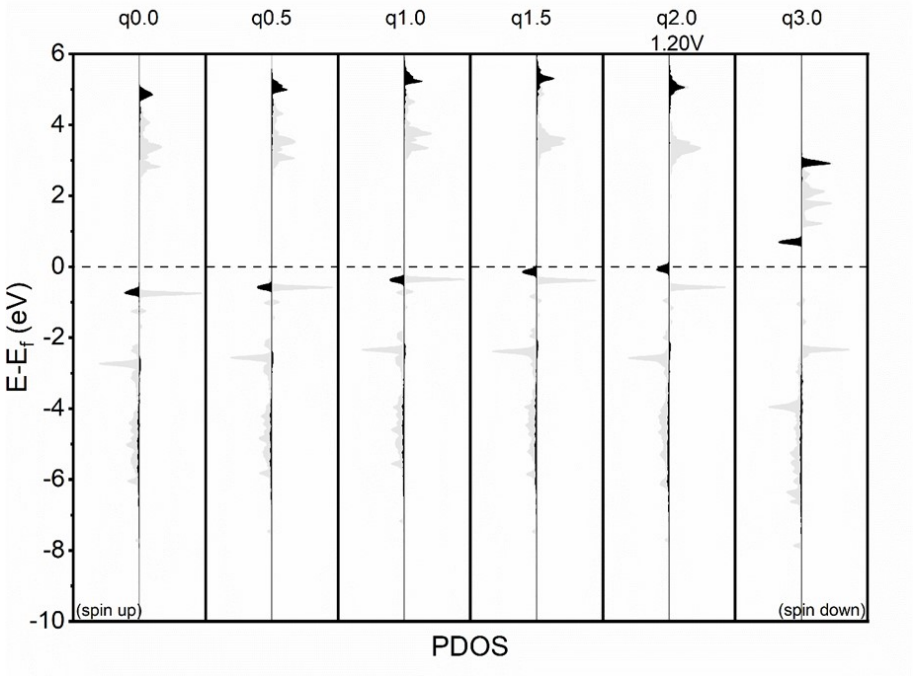


**Fig. S23** PDOS of $FeN_4^{IS}OOH$ (S=2) with removal different charges at 4% strain. (black and grey represent $d_{xy}$ orbital and sum of *d* orbital)

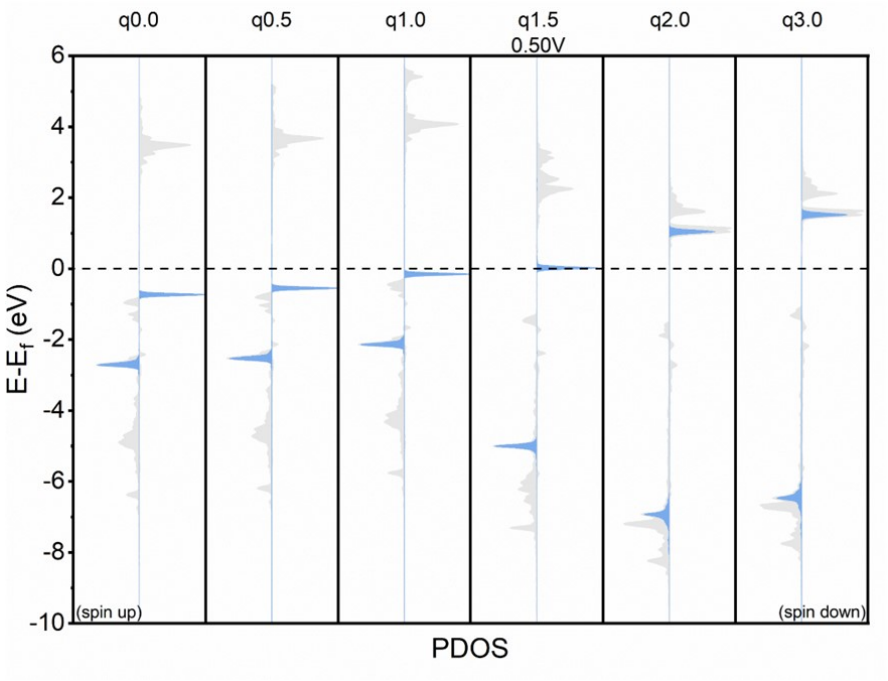


**Fig. S24** PDOS of $FeN_4^{IS}OH$ (S=2) with removal different charges at 8% strain. (blue and grey represent $d_{x2-y2}$ orbital and sum of *d* orbital)

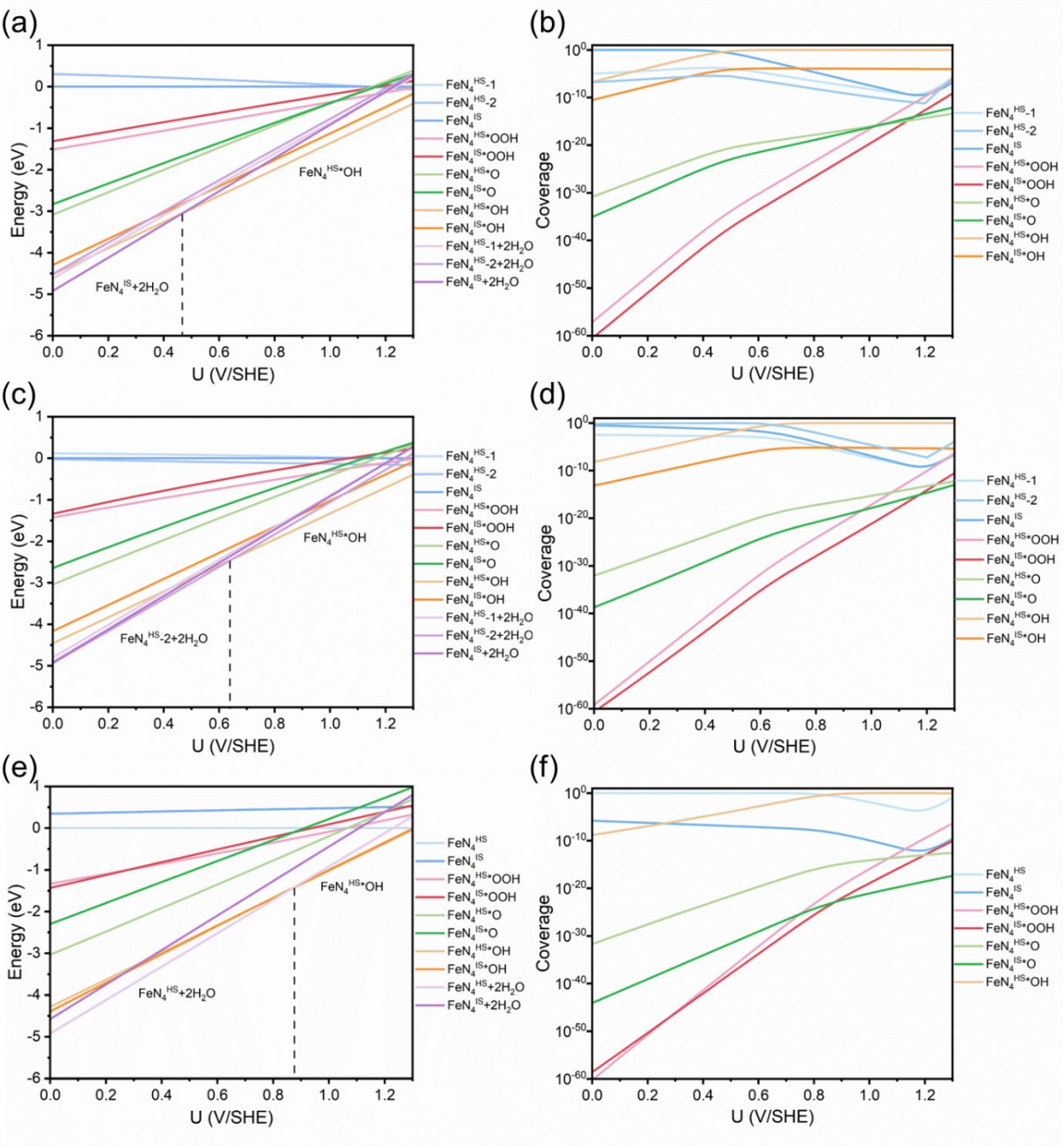


**Fig. S25** Relative energy (refer to $FeN_4^{IS}$) on different voltage (left) and coverage of reaction immediate (right) under different strain. (a-b) 0% strain (c-d) 4% strain, (e-f) 8% strain.

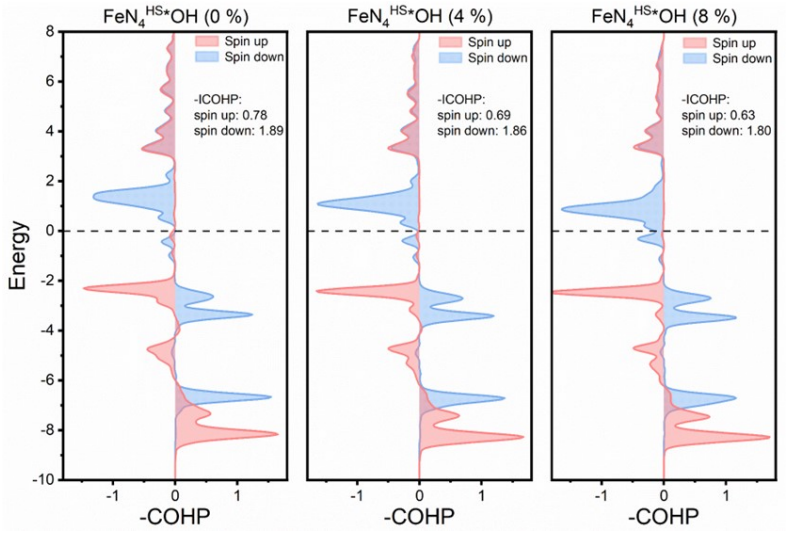


**Fig. S26** COHP analysis for the Fe-O bond between the center Fe and adsorbed *OH in neutral $FeN_4^{HS}$*OH under 0%, 4% and 8% strain.

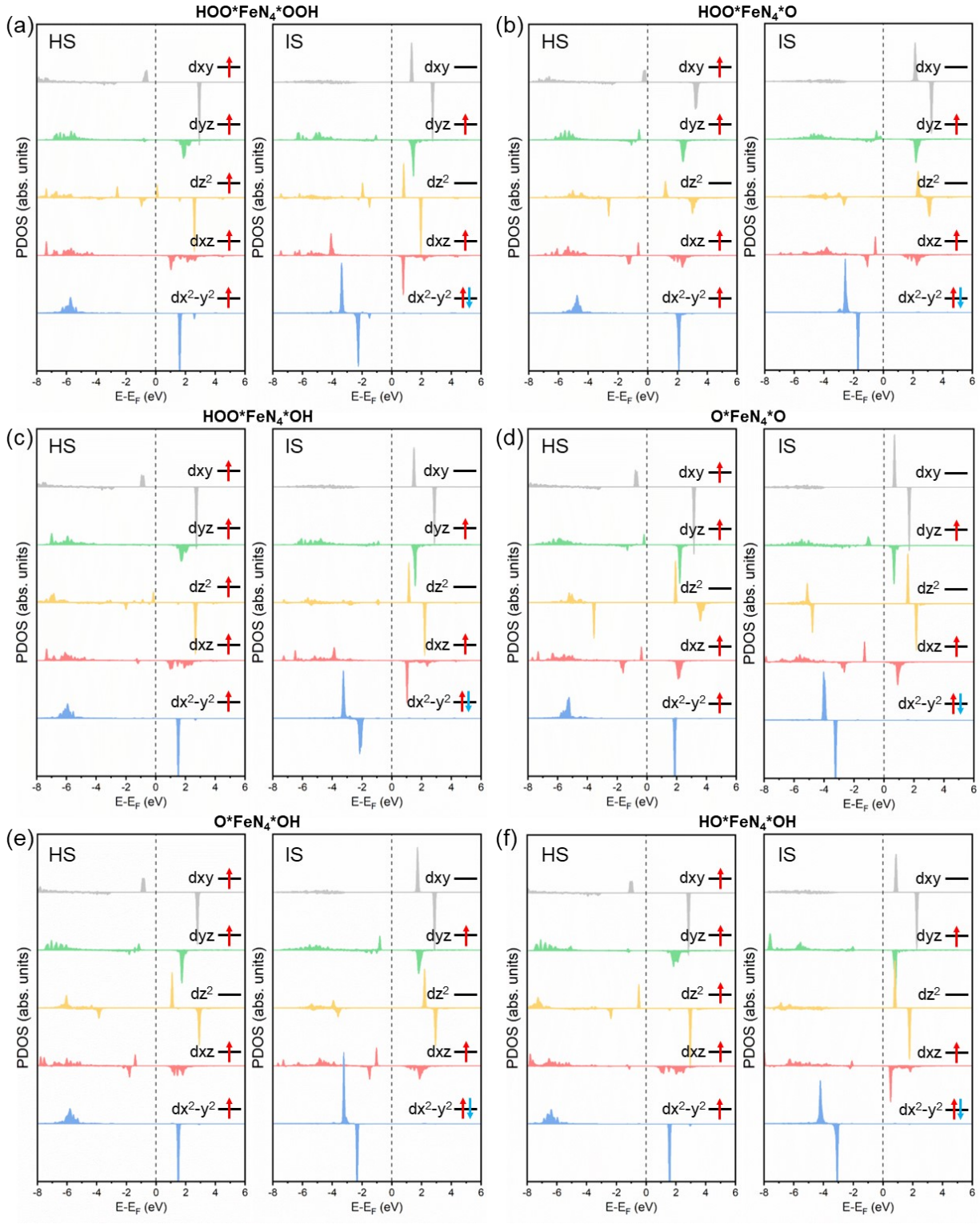


**Fig. S27** PDOS of intermediates and orbital occupation.

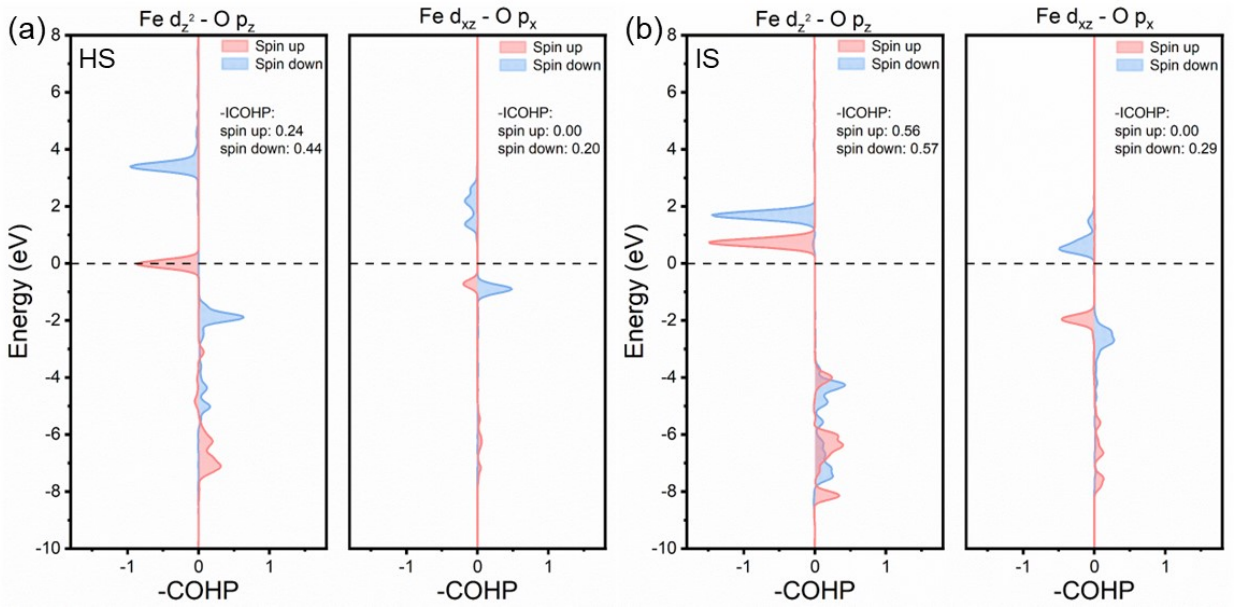


**Fig. S28** Orbital resolved COHP analysis for the Fe-O bond in HO*$FeN_4$*OH with HS state and IS state.

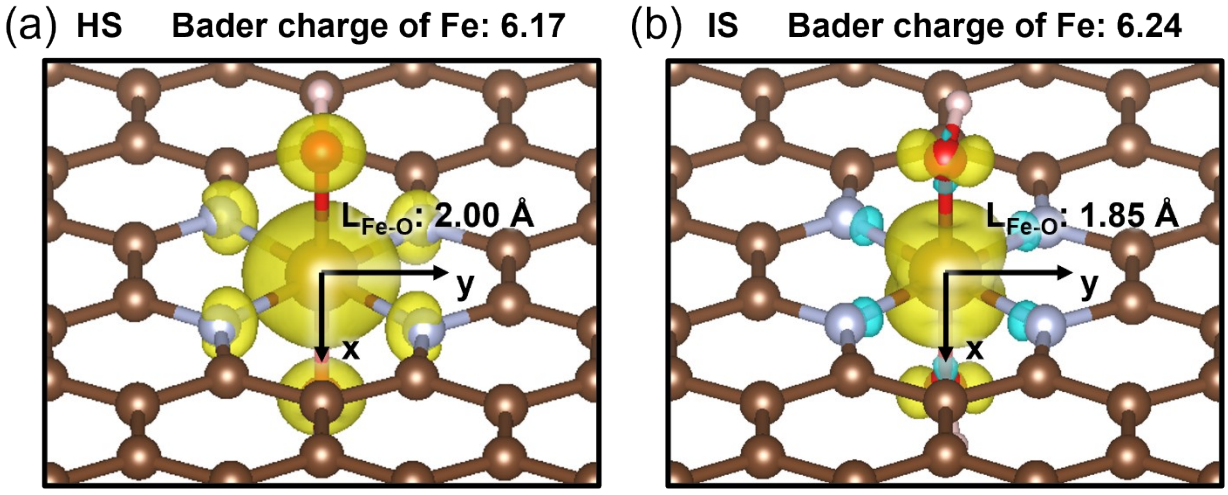


**Fig. S29** Spin charge density of HO*$FeN_4$*OH with HS/IS, bond length of Fe-O and Bader charge of Fe is also given.

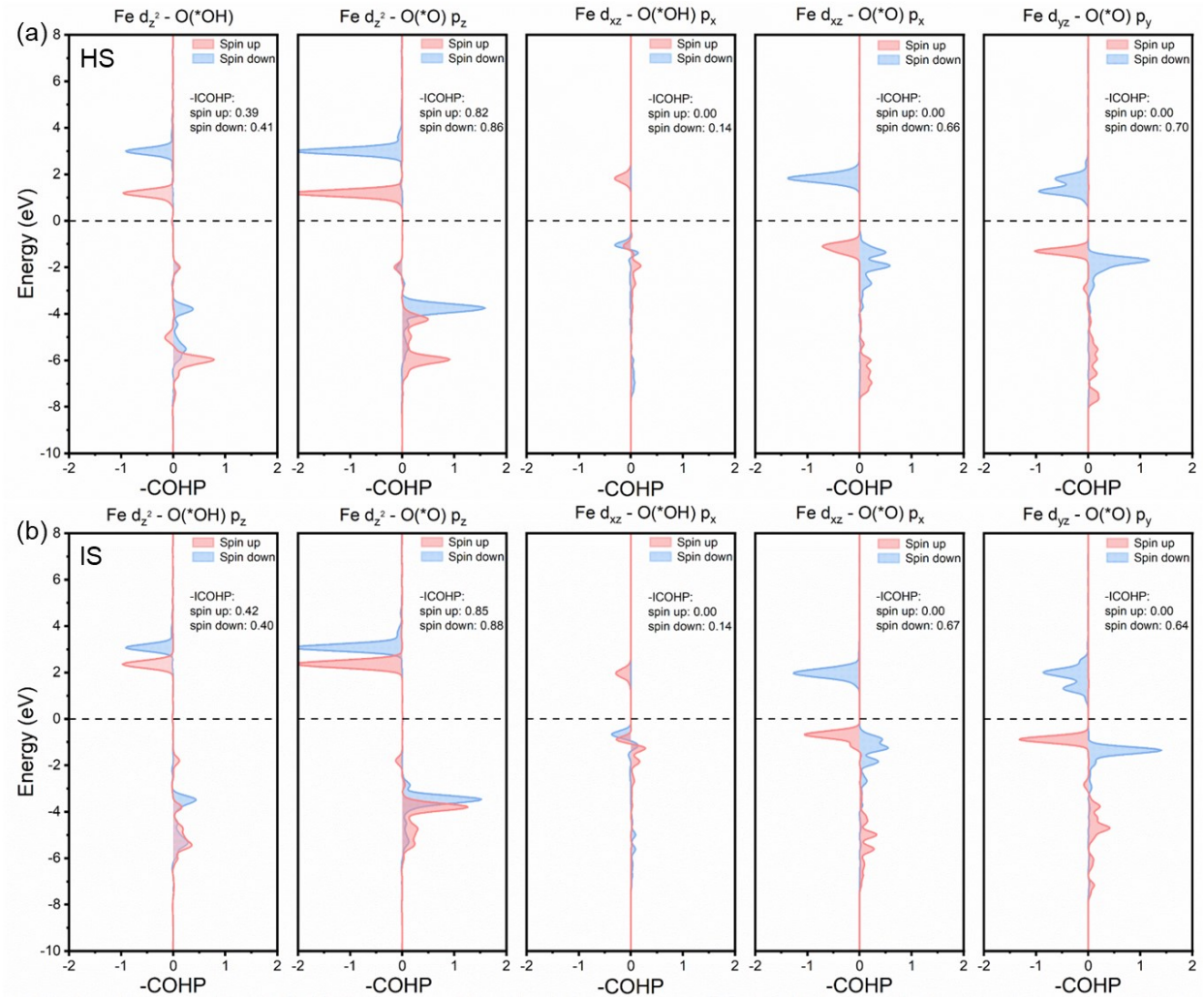


**Fig. S30** Orbital resolved COHP analyze for the Fe-O bond in O*$FeN_4$*HO. (a) HS, (b) IS.

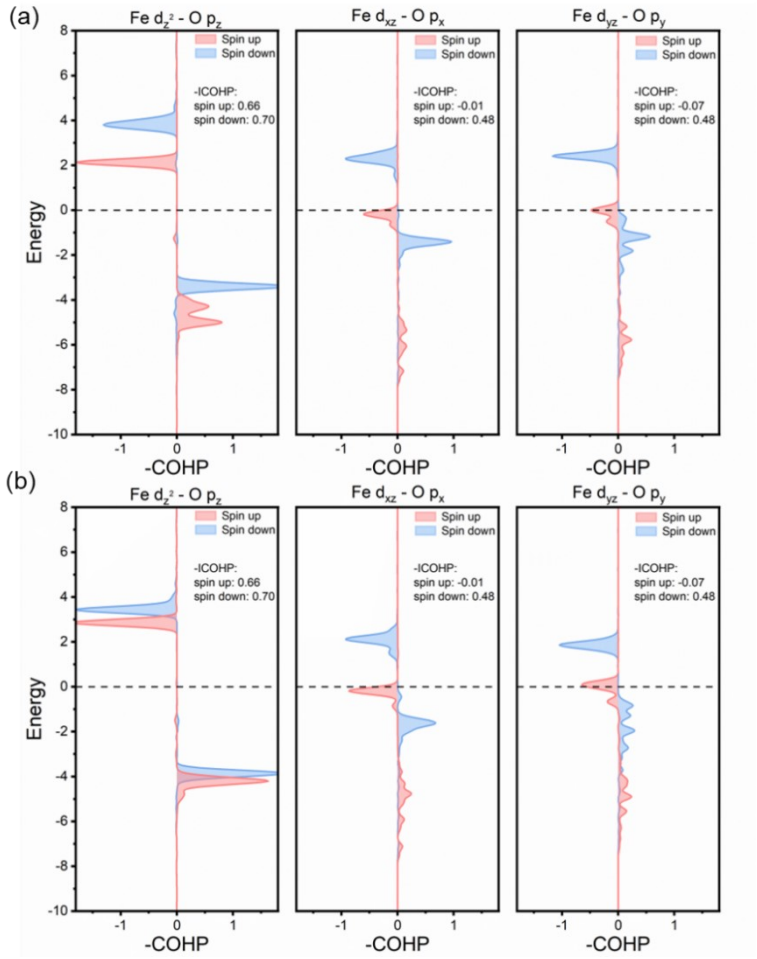


**Fig. S31** Orbital resolved COHP analyze for the Fe-O bond in O*$FeN_4$*O. (a) HS, (b) IS.

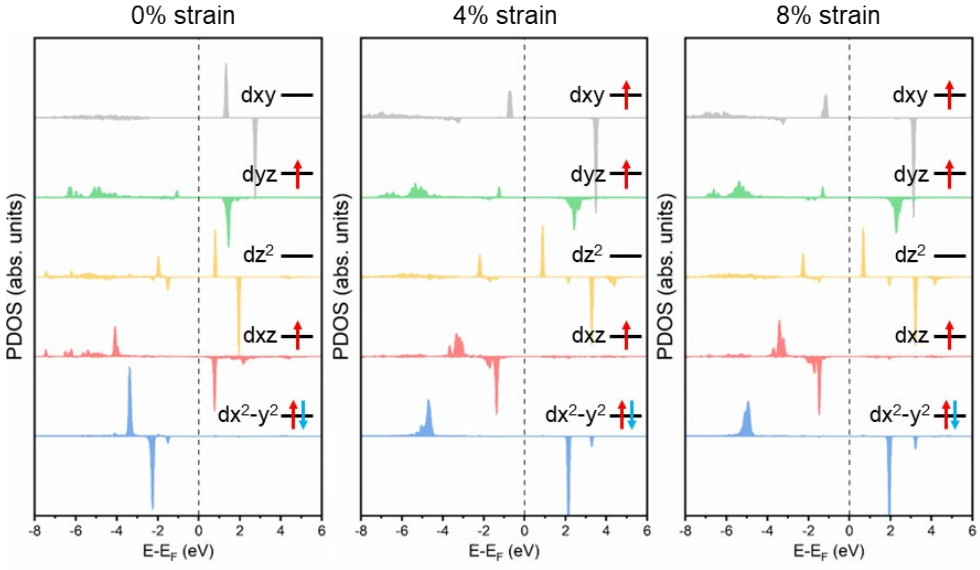


**Fig. S32** PDOS of HOO*$FeN_4^{IS}$*OOH under 0%, 4% and 8% strain.

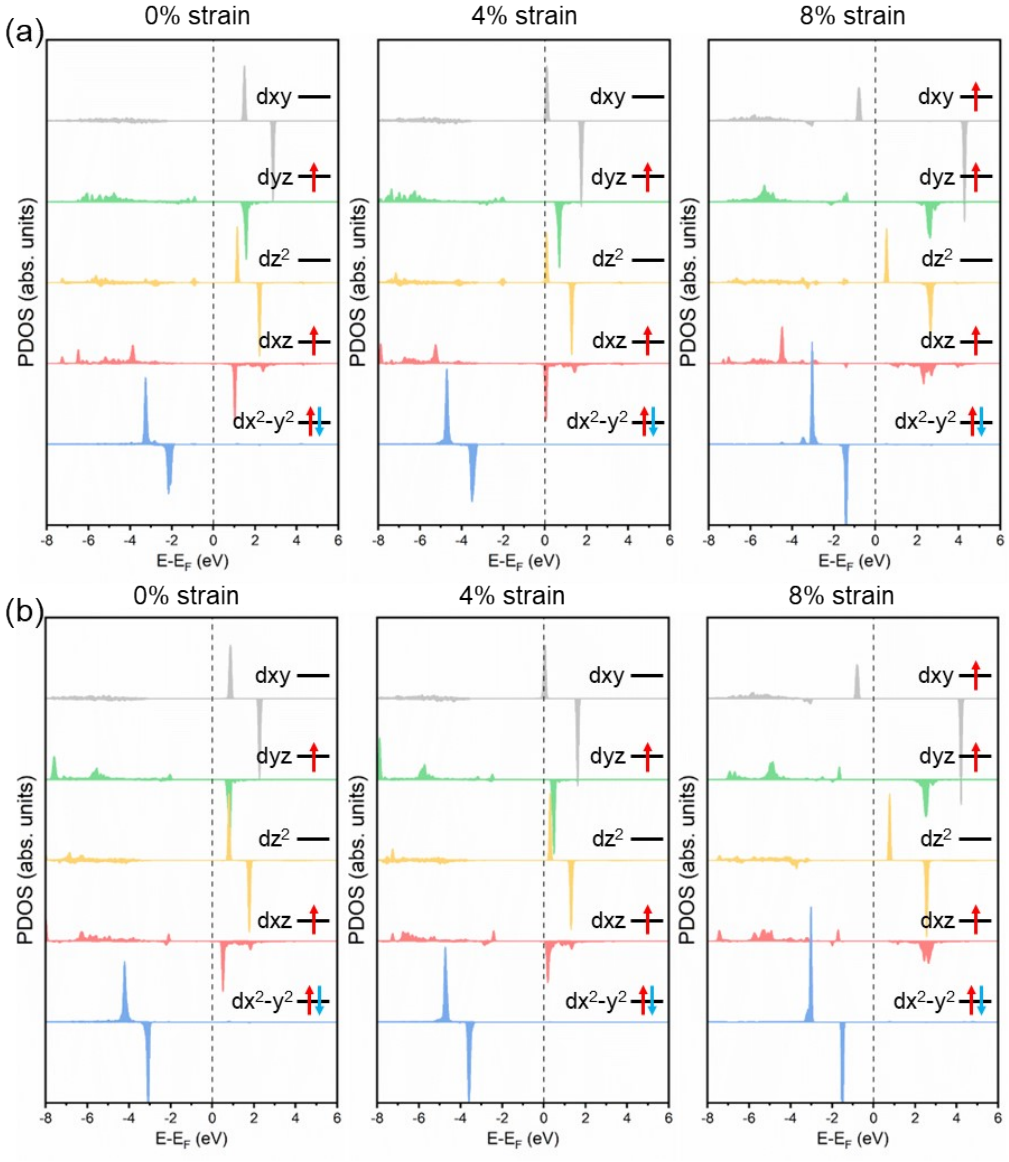


**Fig. S33** PDOS of (a) HO*$FeN_4^{IS}$*OOH and (b) HO*$FeN_4^{IS}$*OH and under 0%, 4% and 8% strain.

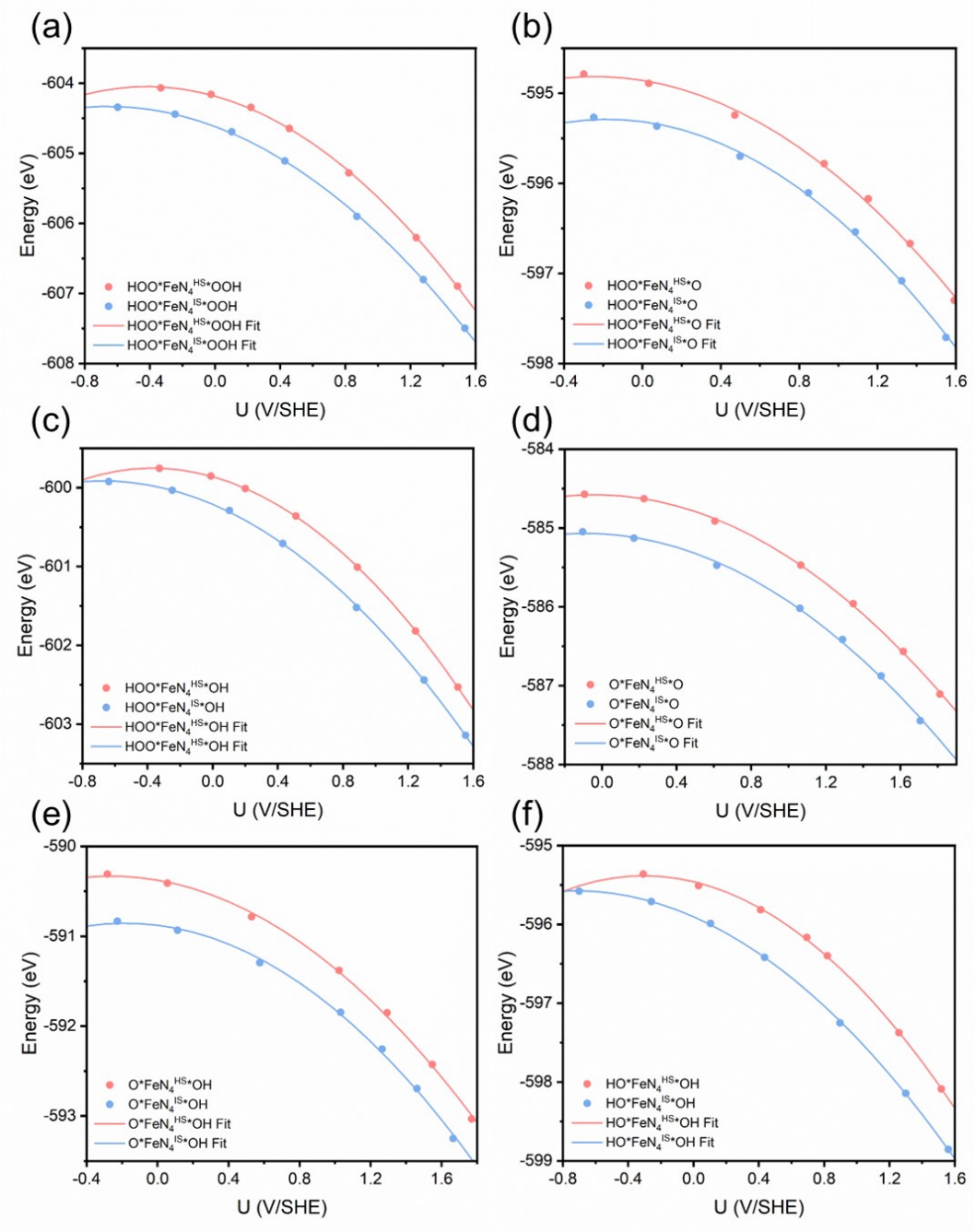


**Fig. S34** Potential-dependent free energy of different spin state of (a) HOO*$FeN_4$*OOH, (b) HOO*$FeN_4$*O, (c) HOO*$FeN_4$*OH, (d) O*$FeN_4$*O, (e) O*$FeN_4$*OH and (f) HO*$FeN_4$*OH under 0% strain.

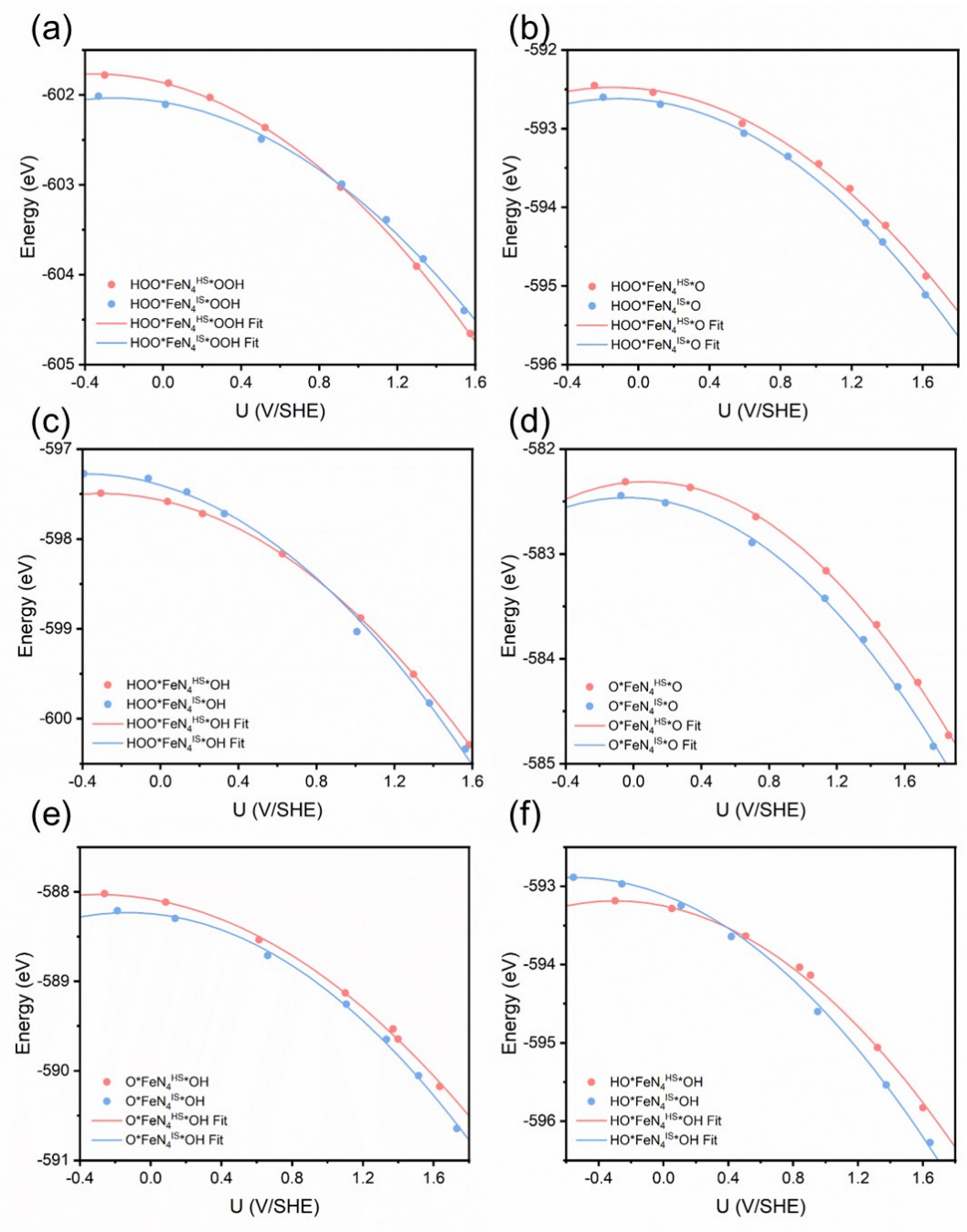


**Fig. S35** Potential-dependent free energy of different spin state of (a) HOO*$FeN_4$*OOH, (b) HOO*$FeN_4$*O, (c) HOO*$FeN_4$*OH, (d) O*$FeN_4$*O, (e) O*$FeN_4$*OH and (f) HO*$FeN_4$*OH under 4% strain.

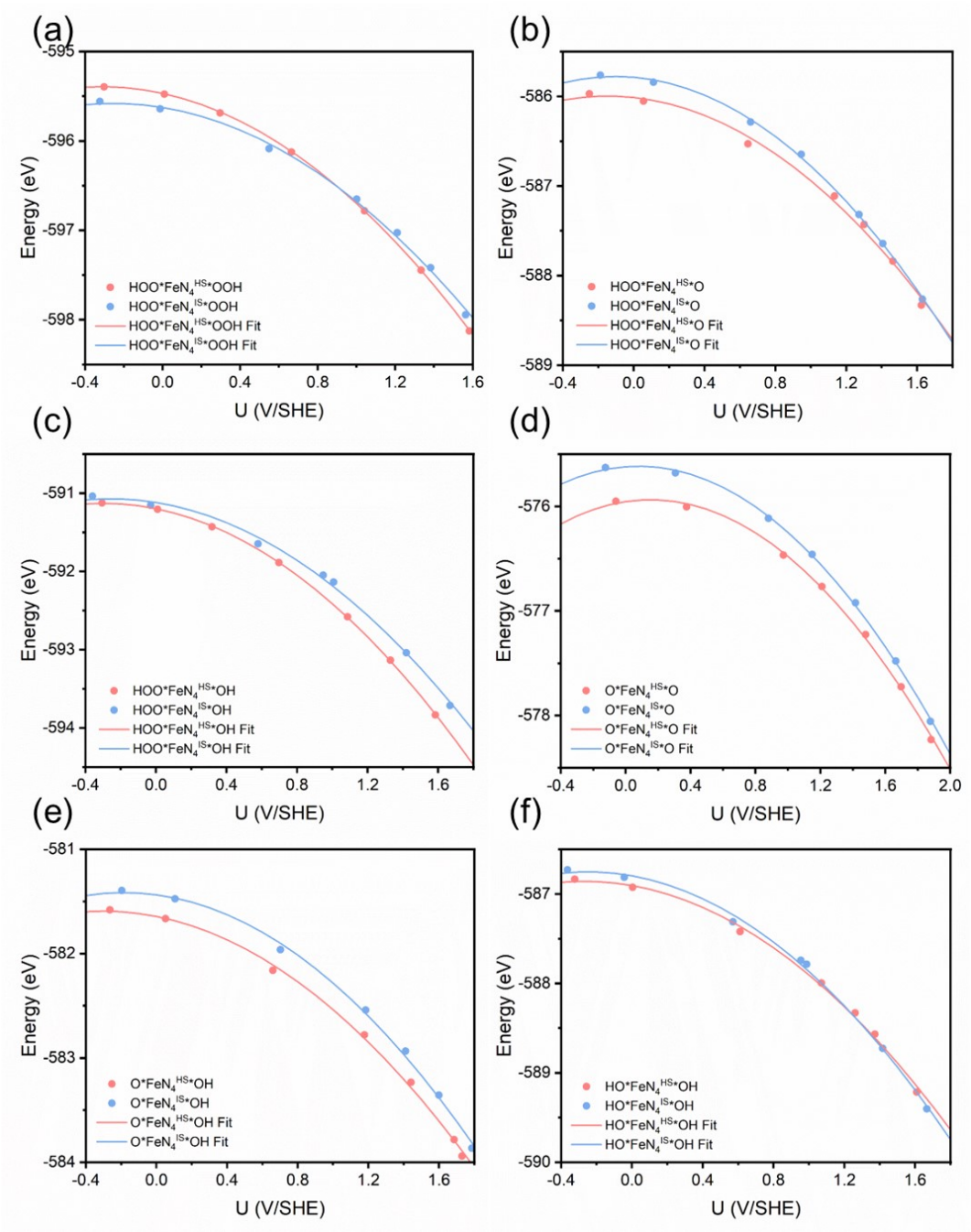


**Fig. S36** Potential-dependent free energy of different spin state of (a) HOO*$FeN_4$*OOH, (b) HOO*$FeN_4$*O, (c) HOO*$FeN_4$*OH, (d) O*$FeN_4$*O, (e) O*$FeN_4$*OH and (f) HO*$FeN_4$*OH under 8% strain.

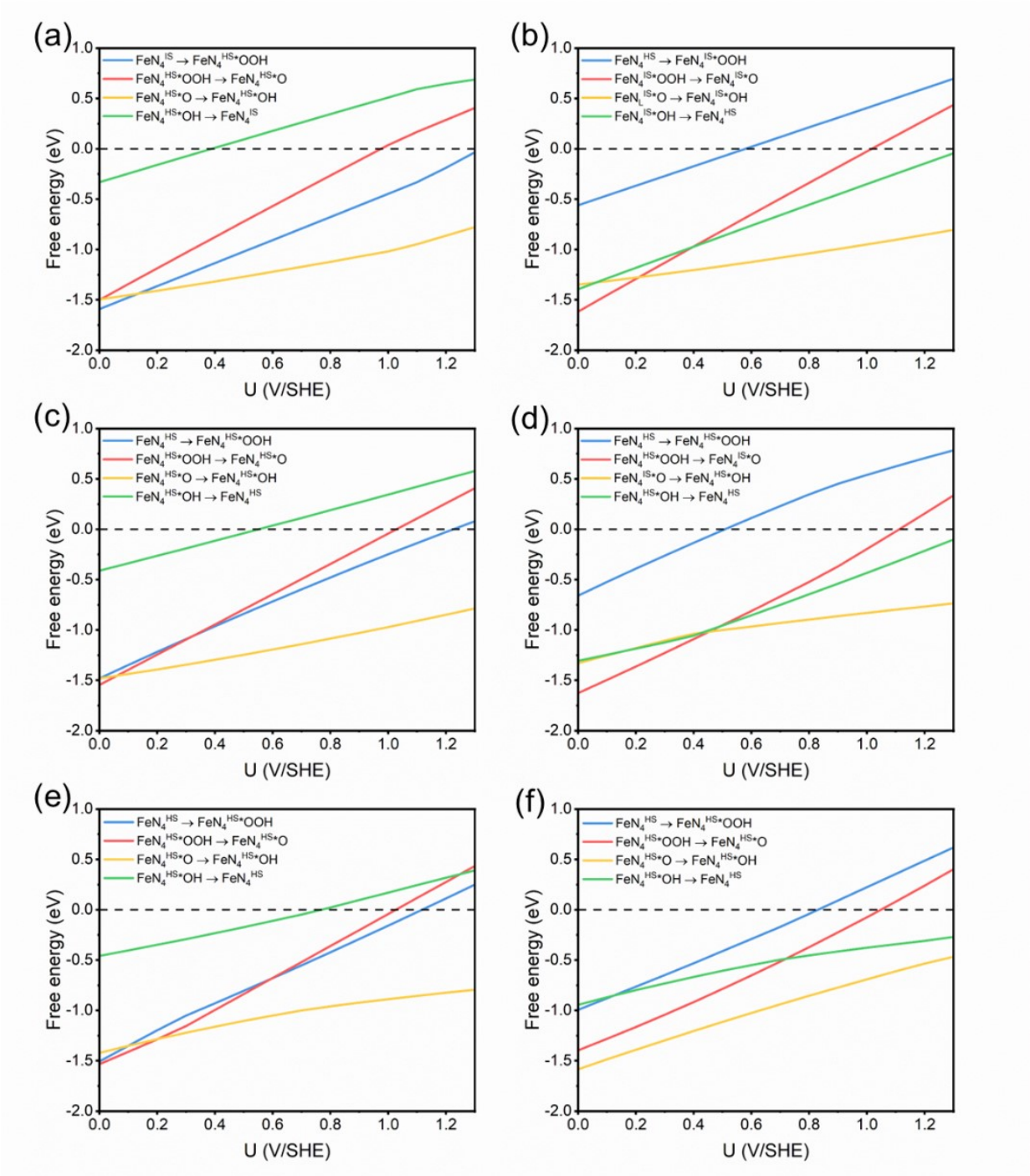


**Fig. S37** ORR reaction free energy in $FeN_4^{IS/HS}$ (left) and $FeN_4^{HS}$*OH (right) under different strain. (a-b) 0% strain, (c-d) 4% strain, (e-f) 8% strain.

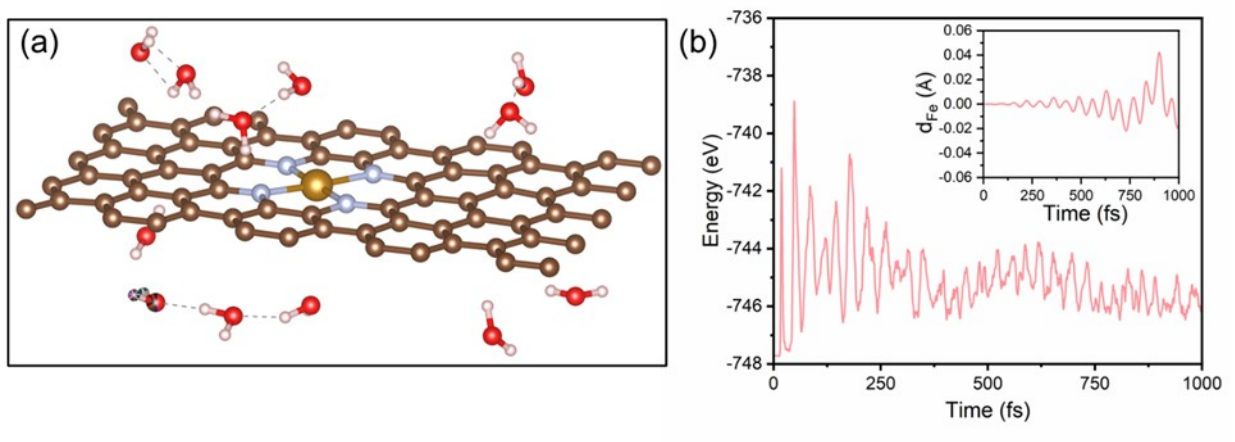


**Fig. S38** (a) Structure of FeN4IS with explicit solvation. (b) AIMD simulation result of $FeN_4^{IS}$ with explicit solvation at 300K for 1 ps (Insert: out-plane displacement of Fe refers to N).

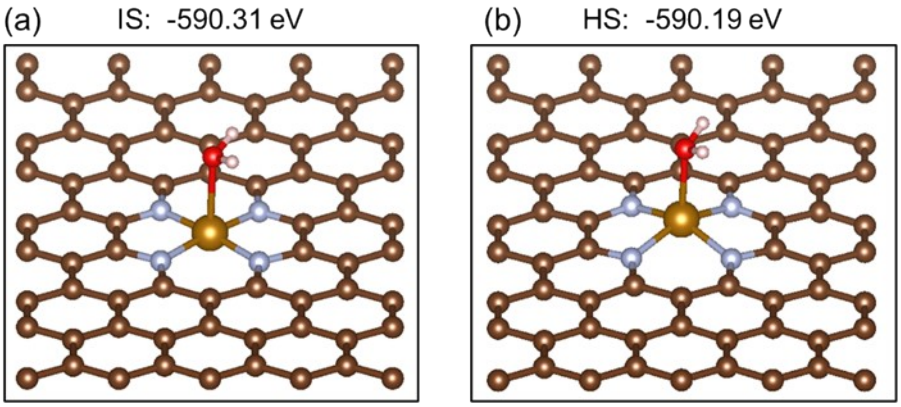


**Fig. S39** Structure of (a) $FeN_4^{IS}$*$H_2O$ and (b) $FeN_4^{HS}$*$H_2O$. (Top: Free energy calculated by implicit solvation model)

**Table S1.** Fitted parameters of quadratic equation for calculating the total energies of various models, spin multiplicity and thermodynamic correction under 0% strain.

| model | Spin | C (e/V) | $U_0$ (V/SHE) | $E_0$ (eV) | $E_{ZPE}$-T*S (eV) |
|---|---|---|---|---|---|
| $FeN_4^{HS}$-1 | 2 | 1.49 | -0.78 | -574.95 | 0.54 |
| $FeN_4^{HS}$-2 | 2 | 1.50 | -0.78 | -574.94 | 0.54 |
| $FeN_4^{IS}$ | 1 | 1.33 | -0.74 | -575.33 | 0.54 |
| $FeN_4^{HS}$*OOH | 5/2 | 1.31 | -0.65 | -590.26 | 0.87 |
| $FeN_4^{IS}$*OOH | 3/2 | 1.40 | -0.59 | -590.09 | 0.87 |
| $FeN_4^{HS}$*O | 2 | 1.39 | -0.20 | -581.11 | 0.58 |
| $FeN_4^{IS}$*O | 1 | 1.47 | -0.33 | -580.81 | 0.58 |
| $FeN_4^{HS}$*OH | 5/2 | 1.29 | -0.66 | -586.03 | 0.86 |
| $FeN_4^{IS}$*OH | 3/2 | 1.28 | -0.66 | -585.80 | 0.86 |
| HOO*$FeN_4^{HS}$*OOH | 3 | 1.57 | -0.42 | -604.05 | 1.32 |
| HOO*$FeN_4^{IS}$*OOH | 1 | 1.32 | -0.66 | -604.33 | 1.32 |
| HOO*$FeN_4^{HS}$*O | 2 | 1.47 | -0.24 | -594.81 | 1.00 |
| HOO*$FeN_4^{IS}$*O | 1 | 1.60 | -0.18 | -595.29 | 1.00 |
| HOO*$FeN_4^{HS}$*OH | 3 | 1.58 | -0.37 | -599.75 | 1.30 |
| HOO*$FeN_4^{IS}$*OH | 1 | 1.30 | -0.68 | -599.91 | 1.30 |
| O*$FeN_4^{HS}$*O | 2 | 1.46 | -0.04 | -584.58 | 0.63 |
| O*$FeN_4^{IS}$*O | 1 | 1.45 | -0.09 | -585.07 | 0.63 |
| O*$FeN_4^{HS}$*OH | 2 | 1.28 | -0.27 | -590.33 | 0.96 |
| O*$FeN_4^{IS}$*OH | 1 | 1.38 | -0.18 | -580.56 | 0.96 |
| HO*$FeN_4^{HS}$*OH | 3 | 1.63 | -0.30 | -595.38 | 1.24 |
| HO*$FeN_4^{IS}$*OH | 1 | 1.26 | -0.72 | -595.57 | 1.24 |

**Table S2.** Fitted parameters of quadratic equation for calculating the total energies of various models, spin multiplicity and thermodynamic correction under 4% strain.

| model | Spin | C (e/V) | $U_0$ (V/SHE) | $E_0$ (eV) | $E_{ZPE}$-T*S (eV) |
|---|---|---|---|---|---|
| $FeN_4^{HS}$-1 | 2 | 1.37 | -0.75 | -572.51 | 0.54 |

| | | | | | |
|---|---|---|---|---|---|
| $FeN_4^{HS}$-2 | 2 | 1.25 | -0.88 | -572.55 | 0.54 |
| $FeN_4^{IS}$ | 1 | 1.28 | -0.76 | -572.64 | 0.54 |
| $FeN_4^{HS}$*OOH | 5/2 | 1.46 | -0.53 | -587.57 | 0.84 |
| $FeN_4^{IS}$*OOH | 2 | 1.69 | -0.30 | -587.60 | 0.86 |
| $FeN_4^{HS}$*O | 2 | 1.46 | -0.19 | -578.39 | 0.54 |
| $FeN_4^{IS}$*O | 1 | 1.62 | -0.26 | -577.96 | 0.56 |
| $FeN_4^{HS}$*OH | 5/2 | 1.30 | -0.65 | -583.29 | 0.84 |
| $FeN_4^{IS}$*OH | 3/2 | 1.28 | -0.65 | -583.00 | 0.85 |
| HOO*$FeN_4^{HS}$*OOH | 3 | 1.56 | -0.36 | -601.76 | 1.20 |
| HOO*$FeN_4^{IS}$*OOH | 3/2 | 1.44 | -0.25 | -602.03 | 1.25 |
| HOO*$FeN_4^{HS}$*O | 2 | 1.52 | -0.14 | -592.47 | 0.97 |
| HOO*$FeN_4^{IS}$*O | 1 | 1.65 | -0.12 | -592.62 | 0.99 |
| HOO*$FeN_4^{HS}$*OH | 3 | 1.56 | -0.31 | -597.49 | 1.23 |
| HOO*$FeN_4^{IS}$*OH | 1 | 1.63 | -0.39 | -597.27 | 1.26 |
| O*$FeN_4^{HS}$*O | 2 | 1.50 | 0.07 | -582.31 | 0.61 |
| O*$FeN_4^{IS}$*O | 1 | 1.43 | -0.04 | -582.46 | 0.63 |
| O*$FeN_4^{HS}$*OH | 2 | 1.12 | -0.30 | -588.03 | 0.92 |
| O*$FeN_4^{IS}$*OH | 1 | 1.36 | -0.13 | -588.23 | 0.94 |
| HO*$FeN_4^{HS}$*OH | 3 | 1.43 | -0.30 | -593.19 | 1.21 |
| HO*$FeN_4^{IS}$*OH | 1 | 1.43 | -0.55 | -592.89 | 1.23 |

**Table S3.** Fitted parameters of quadratic equation for calculating the total energies of various models, spin multiplicity and thermodynamic correction under 8% strain.

| model | Spin | C (e/V) | $U_0$ (V/SHE) | $E_0$ (eV) | $E_{ZPE}$-T*S (eV) |
|---|---|---|---|---|---|
| $FeN_4^{HS}$-2 | 2 | 1.50 | -0.70 | -566.00 | 0.55 |
| $FeN_4^{IS}$ | 1 | 1.51 | -0.61 | -565.76 | 0.54 |
| $FeN_4^{HS}$*OOH | 5/2 | 1.49 | -0.53 | -576.54 | 0.82 |
| $FeN_4^{IS}$*OOH | 2 | 1.65 | -0.36 | -576.76 | 0.84 |
| $FeN_4^{HS}$*O | 2 | 1.33 | -0.23 | -571.73 | 0.53 |

| | | | | | |
|---|---|---|---|---|---|
| $FeN_4^{IS}$*O | 1 | 1.47 | -0.37 | -570.93 | 0.55 |
| $FeN_4^{HS}$*OH | 5/2 | 1.33 | -0.67 | -580.73 | 0.83 |
| $FeN_4^{IS}$*OH | 2 | 1.54 | -0.33 | -581.05 | 0.84 |
| HOO*$FeN_4^{HS}$*OOH | 3 | 1.51 | -0.31 | -595.40 | 1.16 |
| HOO*$FeN_4^{IS}$*OOH | 3/2 | 1.39 | -0.26 | -595.58 | 1.23 |
| HOO*$FeN_4^{HS}$*O | 2 | 1.43 | -0.15 | -586.00 | 0.95 |
| HOO*$FeN_4^{IS}$*O | 1 | 1.64 | -0.10 | -585.78 | 0.97 |
| HOO*$FeN_4^{HS}$*OH | 3 | 1.52 | -0.30 | -591.13 | 1.18 |
| HOO*$FeN_4^{IS}$*OH | 3/2 | 1.40 | -0.26 | -591.07 | 1.24 |
| O*$FeN_4^{HS}$*O | 2 | 1.51 | -0.15 | -575.94 | 0.59 |
| O*$FeN_4^{IS}$*O | 1 | 1.49 | 0.08 | -575.62 | 0.61 |
| O*$FeN_4^{HS}$*OH | 2 | 1.11 | -0.30 | -581.59 | 0.91 |
| O*$FeN_4^{IS}$*OH | 1 | 1.23 | -0.19 | -581.41 | 0.93 |
| HO*$FeN_4^{HS}$*OH | 3 | 1.30 | -0.27 | -586.86 | 1.19 |
| HO*$FeN_4^{IS}$*OH | 3/2 | 1.43 | -0.25 | -586.75 | 1.21 |

**Table S4.** Free energy values and thermodynamic correction values of $H_2(g)$, $H_2O(l)$ and $O_2$.

| model | E(eV) | $E_{ZPE}$ | $-T*S+C_p(T)$ | G(eV) |
|---|---|---|---|---|
| $H_2(g)$ | -6.77 | 0.27 | -0.40 | -6.90 |
| $H_2O(l)$ | -14.22 | 0.57 | -0.48 | -14.13 |
| $O_2$ | | | | -9.54 |

**Table S5** Fe-O bond lengths and Fe-O-(H/OH) bond angles in all adsorbed states with HS and IS.

| | $FeN_4$*OOH (S=5/2,3/2) | $FeN_4$*O (S=2,1) | $FeN_4$*OH (S=5/2,3/2) |
|---|---|---|---|
| HS | 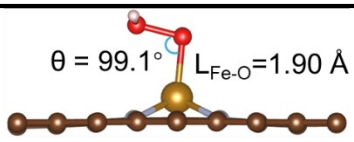 | 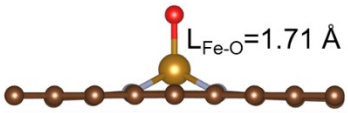 | 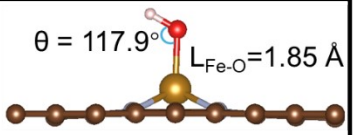 |
| IS | 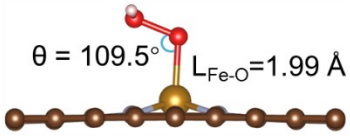 | 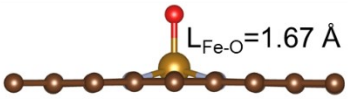 | 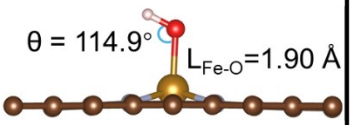 |
| | **HOO*$FeN_4$*OOH (S=5/2,1)** | **HOO*$FeN_4$*O (S=2,1)** | **HOO*$FeN_4$*OH (S=5/2,1)** |
| HS | 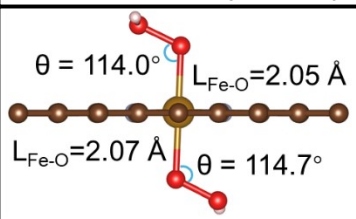 | 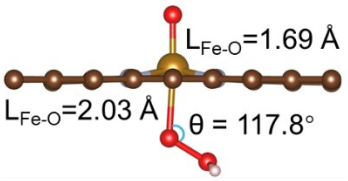 | 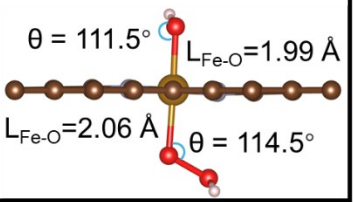 |
| IS | 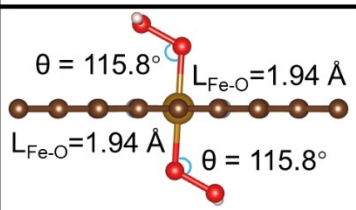 | 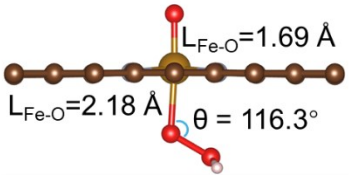 | 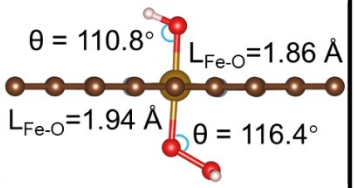 |
| | **O*$FeN_4$*O (S=2,1)** | **O*$FeN_4$*OH (S=2,1)** | **HO*$FeN_4$*OH (S=5/2,1)** |
| HS | 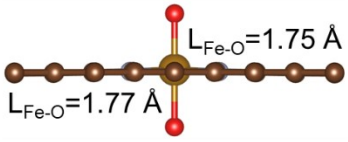 | 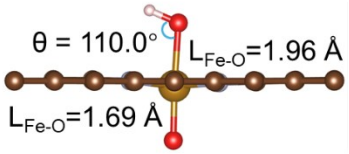 | 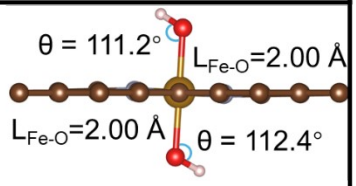 |
| IS | 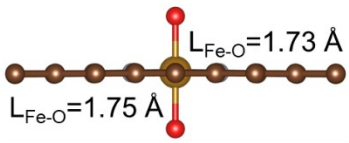 | 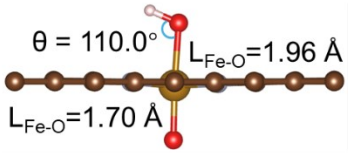 | 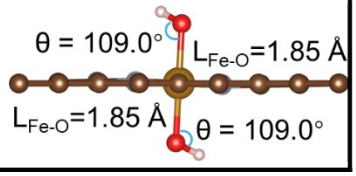 |

**References:**


1. J. K. Nørskov, J. Rossmeisl, A. Logadottir, L. Lindqvist, J. R. Kitchin, T. Bligaard and H. Jonsson, *J. Phys. Chem. B* . 2004, **108**, 17886-17892.
2. I. C. Man, H. Y. Su, F. Calle-Vallejo, H. A. Hansen, J. I. Martínez, N. G. Inoglu, J. Kitchin, T. F. Jaramillo, J. K. Nørskov and J. Rossmeisl, *ChemCatChem*, 2011, **3**, 1159-1165.
3. M. Li, L. Zhang, Q. Xu, J. Niu and Z. Xia, *J. Catal.*, 2014, **314**, 66-72.
4. Y. Ping, R. J. Nielsen and W. A. Goddard III, *J. Am. Chem. Soc.*, 2017, **139**, 149-155.
5. Y. Wang, Y. J. Tang and K. Zhou, *J. Am. Chem. Soc.*, 2019, **141**, 14115-14119.
6. D. T. Limmer, A. P. Willard, P. Madden and D. Chandler, *Proc. Natl. Acad. Sci.*, 2013, **110**, 4200-4205.
7. Z. Huang and Q. Tang, *J. Phys. Chem. C* . 2022, **126**, 21606-21615.
8. H. A. Hansen, V. Viswanathan and J. K. Nørskov, *J. Phys. Chem. C* . 2014, **118**, 6706-6718.